AIR FORCE INSTITUTE OF TECHNOLOGY

AIR UNIVERSITY
UNITED STATES AIR FORCE

64-4

SCHOOL OF ENGINEERING

WRIGHT—PATTERSON AIR FORCE BASE, OHIO

AF-WP-O-OCT 62 3,500

PROJECT HOTSHOT -

PARTICLE THERMAL RADIATOR

Capt Alfred H. Davidson III

Capt James F. Russell

GA/Phys/63-1,9

AF-WP-O-SEP 63 30

PROJECT HOT SHOT -
PARTICLE THERMAL RADIATOR

THESIS

Presented to the Faculty of the School of Engineering of
the Air Force Institute of Technology
Air University
in Partial Fulfillment of the
Requirements for the Degree of
Master of Science

By

Alfred Harry Davidson III, B.S.
Captain USAF

and

James Franklin Russell, B.S.
Captain USAF

Graduate Astronautics

August 1963

Preface

This study is a continuation of the analysis of the factors involved in the design of a particle thermal radiator for space vehicles. The basic idea was originally proposed by Dr. William L. Lehmann, Professor and Head, Department of Physics. Major Charles F. Neef presented the basic principles of the conceptual design and derived mathematical equations for each phase of operation. Captain Duane W. Smetana extended and modified Neef's calculations, investigated theoretical problem areas, and suggested areas for experimental work.

Our effort has been expended on an experimental investigation of the particle charging and particle motion problems as enumerated by Smetana, and the optimization of several design parameters by a computer study using our experimental results. It is hoped that the results of this study will suggest a method of verifying the heat transfer assumptions used and lead eventually to a successful working model.

We wish to acknowledge our indebtedness to Dr. W.L. Lehmann for the assistance and advice which he so generously gave to us. In addition, we wish to express our gratitude to the personnel of the Electronic Technology Laboratory, A.S.D., Physics Laboratory, A.F.I.T., and especially to Mr. Harry R. Kremer of the Technical Photographic Division, A.S.D, for their invaluable technical assistance.

Contents

Contents

List of Figures

List of Tables

Abstract

The design of a new type thermal radiator is extended. Micron-sized particles are heated and electrically charged on contact with electrode-spheres and radiate thermal energy during oscillations between spheres. Results of experimentation show that metallic particles will charge and the charge transferred (in coulombs) can be calculated from the empirical formula

$$q = 8.16 \times 10^{-23} d^2 (\rho_E)^{.12} E$$

where d is the particle diameter in microns, ρ_E is the particle electrical resistivity in micro-ohm-cm, and E is the electric field in volts per meter. Oscillatory motion was verified between parallel plates. Design of experimental equipment is discussed. Equations are presented for calculation of radiator specific weight. Results of a computer study indicate, for power levels on the order of ten megawatts, the particle radiator will weigh approximately 16 percent of the weight of the conventional radiator.

List of Symbols

A - Heat-transfer area of the heated electrode.

A_p - Surface area of each particle.

a - Particle acceleration.

B - Proportionality constant.

c_N - Specific heat of liquid sodium.

c_p - Specific heat of the particles.

d - Diameter of the particles in microns.

d' - Mean separation between the inner and outer surfaces of the heated electrode.

D - Separation distance between electrode centers.

E - Electric field.

e - Emissivity of the particles.

F - Particle flow rate in number of particles per second.

G - Weight flow rate of liquid sodium per unit area.

g - Acceleration due to gravity.

h - Heat-transfer coefficient.

I - Current due to charged particles flowing between the electrodes.

K_M - Thermal conductivity of molybdenum.

K_N - Thermal conductivity of liquid sodium.

K_P - Thermal conductivity of the particles.

m - Mass of each particle.

N_T - Total number of particles in the system.

q - Electric charge on each particle.

$\dot{q}$ - Rate of heat loss per particle.

$\dot{Q}$ - Rate of heat loss for the entire system.

r - Radius of particle in meters.

R - Radius of electrode-sphere.

t - Thickness of the outer sphere of the heated electrode.

t_c - Time of contact between particles and electrodes.

t_f - Average time of flight between electrodes.

t_h - Representative time required for a particle to heat from arrival temperature to the temperature of the electrode.

T_A - Temperature of the particles when they arrive on the heated electrode.

T_1 - Temperature of the particles as they leave the heated electrode.

ΔT - Temperature difference between the bulk temperature of the liquid sodium and the outer surface of the heated electrode.

U - Overall heat-transfer coefficient.

v - Velocity of the particle.

V - Operating voltage.

W_E - Weight of the electrical generator.

W_P - Weight of the particles.

W_S - Weight of the electrode-spheres.

W_T - Total weight of the radiator.

ρ_E - Electrical resistivity of the particles.

ρ_M - Density of molybdenum.

ρ_P - Density of the particle.

σ - Stephan Boltzmann constant.

PROJECT HOT SHOT -

PARTICLE THERMAL RADIATOR

I. Introduction

In a space environment, radiation is the only method of heat transfer available for rejection of excess heat. "The economical rejection of heat from space power plants has become an increasingly critical problem in space technology. For power plants above the one megwatt range, the conventional tube-and-header radiator is the heaviest single component. This weight is doubly critical because each extra pound makes vehicle launching and its subsequent maneuvering in space more difficult" (Ref 2:1). Thus a means of severely reducing the weight of conventional space radiators, or alternatively, design of a new type light-weight radiator would represent a major breakthrough in space engineering.

C.F. Neef and D.W. Smetana have presented the concepts of a new type thermal radiator for space vehicles. "Modern technology compares radiators according to specific weight which is determined primarily by the area to volume ratio. For small spherical particles, the area to mass ratio becomes

$$\frac{A}{V} = \frac{4\pi r^2}{\frac{4}{3}\pi r^3} = \frac{3}{r} \qquad (1)$$

It is tempting then to examine the use of particles of extremely small radius as radiators" (Ref 2:1). For a given mass of particles, the total surface area can be made arbitrarily large by decreasing particle radius.

The principles of operation of a device using small particles as radiators are shown in Figure 1. Particles contact the heated electrode-sphere and absorb heat by conduction. A potential difference is maintained between the electrodes so that the particle also becomes charged while in contact with the heated electrode. The electric field between the electrodes forces the charged particle along a path, as it is shown, until it collides with the other sphere. There it will be oppositely charged and forced back toward the heated electrode. During the entire trip, the particle is radiating heat into space. As it contacts the heated electrode, the cycle is repeated.

If the weight advantage gained using particles as radiators is not negated by required structure and electrical system weight, then the particle radiator appears to hold a useful advantage over the conventional radiators. Areas for further investigation are listed by Smetana (Ref 2:38):

1. Charge transfer in vacuum.
2. Heat transfer from sphere to particle and particle to space.
3. Materials for particles and electrodes.
4. Charged particle motion in vacuum.

The purpose of this study is generally to extend Neef's and Smetana's work, and specifically to investigate experimentally, in vacuo, charge transfer to particles and the motion of charged particles in air and vacuo. Particle motion experiments are restricted to motion between

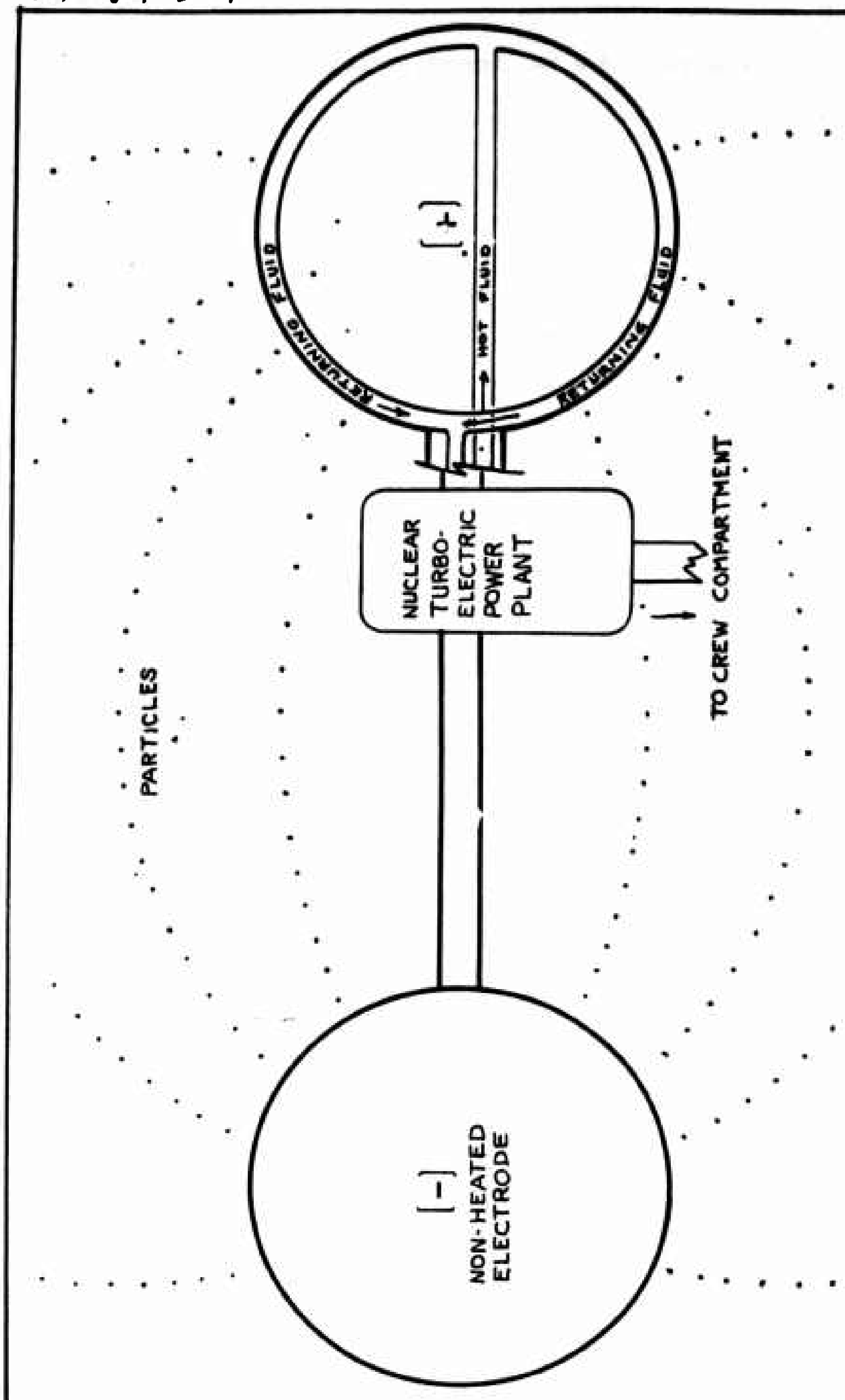

FIGURE 1. Basic Conceptual Design (Ref 2:4)

parallel plates. Results of the two investigations are then used in a computer study to optimize some of the design parameters. No attempt is made to experimentally verify the heat transfer assumptions made by Neef and Smetana. Selection of sphere and particle materials is made on an analytical rather than an experimental basis.

Results show that metallic particles can be charged but dielectric particles cannot. Charging depends on electric field, particle size, and particle material. Charged particle motion is successfully photographed in vacuum at normal gravity and in air at zero gravity. Contact time between particle and plate compares favorably to the time required to heat a particle. The computer design analysis yields a specific weight for the particle radiator on the order of 0.055 kilograms per kilowatt compared to a value on the order of .35 kilograms per kilowatt (Ref 2:36) for a conventional tube-and-header radiator.

II. Charge Measurement

Previous investigations of particle charging have been based upon the use of dielectric particles only (Ref 2:6, 22). For his study, Smetana assumed that the charge, q (coulombs), on a dielectric particle was given by

$$q = 2.4 \times 10^{-16} d^2 \qquad (2)$$

where d is the diameter of the particle in microns (Ref 2:10). Smetana then concludes, "Of all the problems considered, those associated with electrical charging (of particles) in space are potentially the greatest" (Ref 2:23).

In this chapter, a method of experimentally measuring the charge transferred to particles (dielectric or metallic) is described. The following variables are examined for their affect on particle charging: air pressure, electric field, plate material, plate temperature, particle size, particle material, and particle velocity. It is shown that only metallic particles can be charged by contact with a metal plate which has a known electric field at its surface. The three variables that affect charging are found to be electric field, particle size, and particle material. An empirical formula for the charge on a particle is developed from the observed data.

Description of Charge Measuring Apparatus

Figure 2 shows the apparatus that was designed to measure the average charge per particle in a stream of particles (B) falling on the metal plate (A). The particles, formed into a stream by the funnel shown, fall through a hole in the screen (C) and onto the metal plate. The plate then deflects the particles into a metal cup (D) that is connected to the input terminal of a Keithley Model 410 micro-microammeter (E). A D.C. voltage source (not shown) is connected to the plate (A) to provide an electric field between the plate and the grounded screen.

The weight flow rate of particles in the stream was measured by timing the flow through the funnel of a known weight of particles. The flow rate of average sized particles, F, (particles per second) is then calculated by dividing the weight flow rate (kilograms per second) by the average particle weight (kilograms per particle). See the next section for a discussion of average particle weight.

If there is charge transfer between the plate and the particles, the stream of particles will carry a current between the plate and the cup. The magnitude of this current, I , in amperes (coulombs per second) is measured by the micro-microammeter. The average charge per particle, q , (coulombs) is then given by

$$q = \frac{I}{F} \tag{3}$$

Particle Weight and Size

Particles of various sizes existed for all the particle materials used. Therefore, it was necessary to obtain the weight of an average

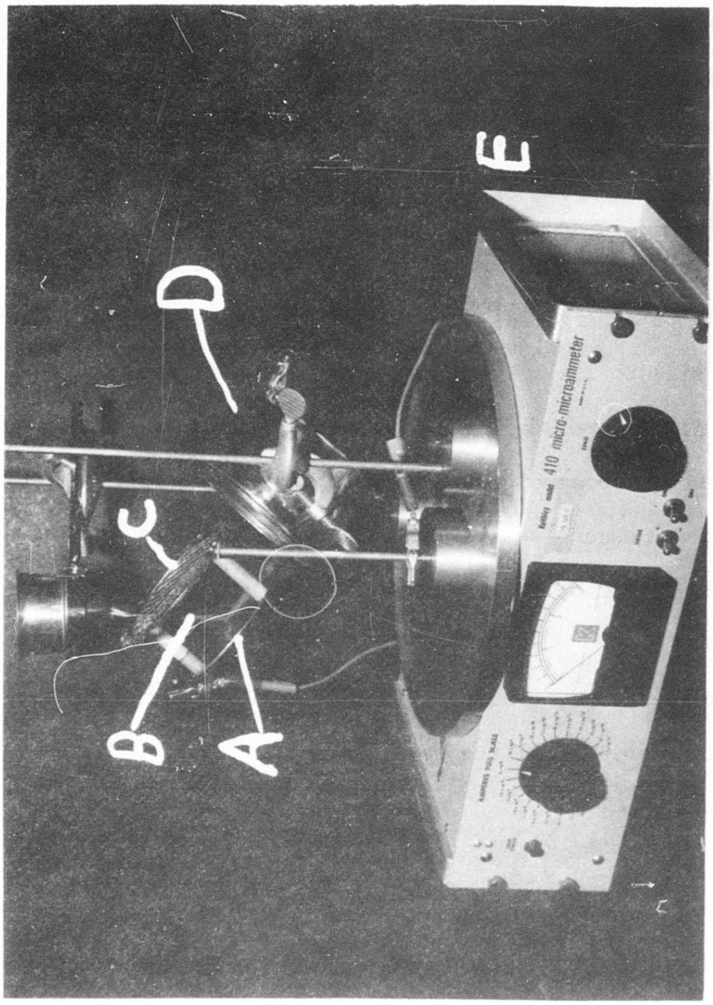

Figure 2

CHARGE MEASURING APPARATUS

particle for each material. The average particle weight was calculated by weighing about 200 particles chosen at random and averaging their weights. A spherical shape was then assumed for each average particle and the diameters of these fictitious spheres were calculated. These average diameters, d, will be used for size comparisons and are listed in Figure 3.

Variables Investigated

Seven variables were investigated to determine how each affected the charge transferred to a particle. Atmospheric pressure was varied from sea level (14.7 psia) to 1×10^{-6} mm Hg which is equivalent to the pressure at 131 miles above sea level. The apparatus shown in Figure 2, except for the micro-microammeter, was placed inside the bell jar of a vacuum system where pressure was varied within the limits specified above. Lower pressures could not be obtained with the vacuum equipment used for this investigation.

The electric field, E, (volts per meter) between the plate and the screen was calculated by use of the potential difference, V, and the separation distance, D

$$E = \frac{V}{D} \tag{4}$$

A separation distance of 0.054 meters was used. The potential difference was varied from -4500 volts to +4500 volts to obtain various electric fields (up to 83,300 volts per meter).

Three different plate materials were used: iron, copper, and aluminum. The plates were all 12.7 centimeters in diameter and 1.5

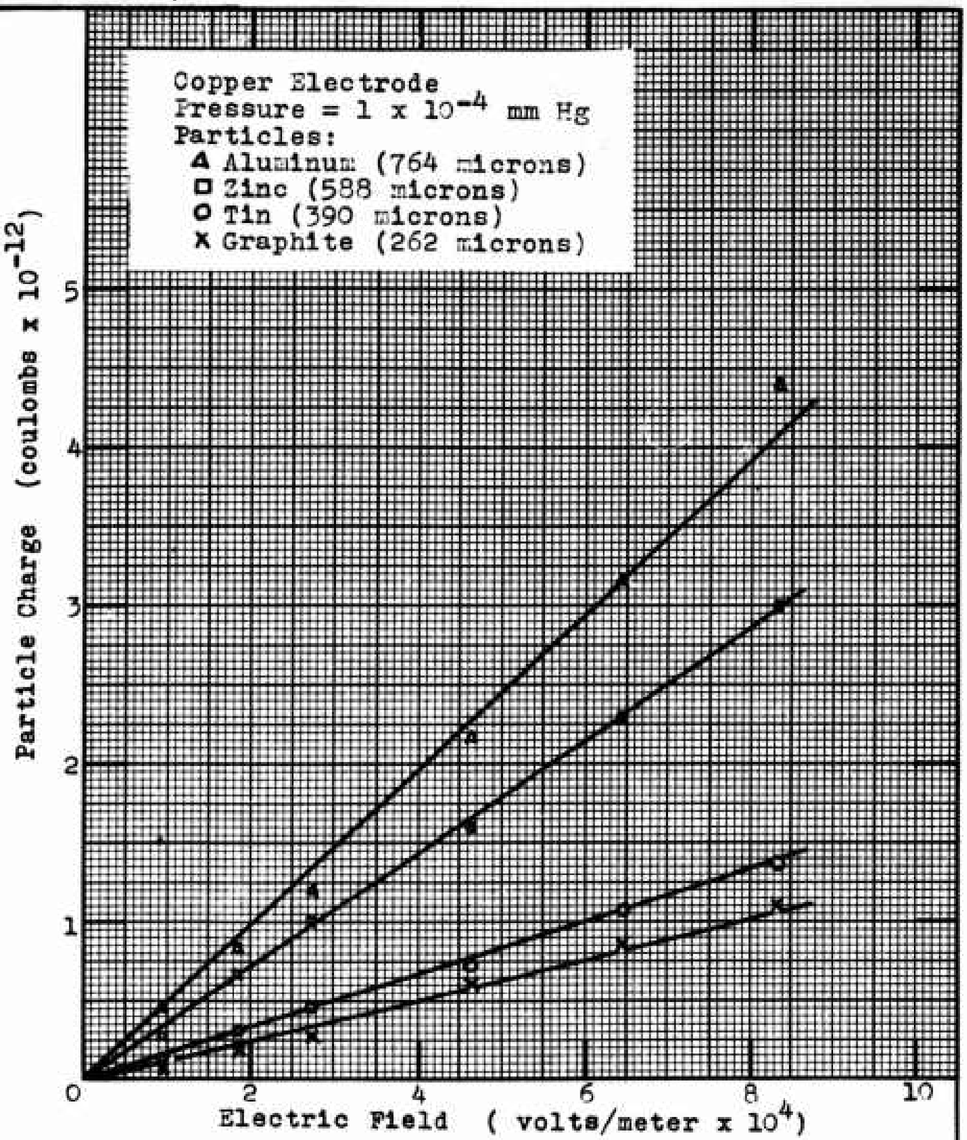

Figure 3

PARTICLE CHARGE

vs

ELECTRIC FIELD

millimeters thick.

Plate temperature was varied in one series of experiments from 293°K to 545°K at atmospheric pressure. A Bunsen burner heated the under side of the plate while an iron-constantine thermocouple measured the temperature of the upper surface.

Charging versus size comparisons were made using two sizes of iron particles.

Particles of aluminum, zinc, tin, graphite, and polystyrene were used to investigate the effect of particle material on charging. The conducting particles were irregular in shape but had smooth surfaces with no sharp edges. The polystyrene particles were generally spherical in shape.

The last variable investigated was particle velocity on impact with the plate. Impact velocity was varied by changing the distance through which the particles fell before contacting the plate.

Charge Measurement Results

The average charge per particle was calculated by using Eq (3). However, it was found that the current measured by the micro-microammeter required a correction factor in order to indicate the true charge transferred to the particles by the electric field. This was necessary because a current was measured with zero potential difference between the plate and the screen while particles were flowing. This current is designated the zero voltage current in this investigation. Zero voltage currents were measured for each type of particle and were algebrically subtracted from the actual readings to obtain the corrected current for use in Eq (3). The sign of the zero voltage current depended on the particle material.

For pressures between the corona discharge value (about 0.025 mm Hg at 500 volts) and 1×10^{-6} mm Hg, there was no measurable difference in particle charging. As pressure was increased from 0.025 mm Hg to standard atmospheric pressure, charging was decreased by less than one-tenth its value at 1×10^{-6} mm Hg. This decrease was caused by charge leaking to the air as particles traveled from plate to cup.

The result of varying the electric field for different particles is shown in Figure 3. The separation distance used for these data was 0.054 meters. It was concluded that charging varies linearly with electric field. Reversing the direction of the electric field reversed the sign of the charge, but had no affect on its magnitude.

Charge variation from using different metal plates (copper, iron, and aluminum) was small compared to the assumed experimental error for the apparatus, particles, and assumptions used. This error was assumed to be ± 15 percent. Plate temperature variations within the limits previously specified (293 °K to 545 °K) produced no charge variation.

Two groups of iron particles with average surface areas in the ratio of two to one were used to examine the effect of particle size on charging. Measured charges were found to be in the same ratio; thus it was assumed that particle charging varied according to the surface area of the particle. These iron particles are not shown in Figure 3 because they had flat surfaces and sharp corners and were not considered a good approximation to the spherical shape assumed for the other particle materials. Extension of this assumption to the other particles suggests that charge is proportional to the diameter squared of the average sized spheres previously assumed for these particles.

Determination of particle material affect on charging was more difficult than for the other variables. Examination of several physical and electrical properties of the various particle materials revealed that electrical resistivity, ρ_E , (micro ohm cm) provided a correlation to the observed data. The effect of resistivity on charging will be discussed in the next section.

The drop distance of the particles was varied by a factor of about 1.9. Dimensions of the bell jar and scattering of particles prohibited further increases in drop distance. Charging was measured at two particle impact velocities: 1.08 meters per second and 1.5 meters per second with aluminum particles. No difference in charging was observed for these two velocities; however, if much higher particle velocities (for example, ten times greater) become necessary for a working radiator model, then further experimentation with higher velocities should be conducted. Within the range of velocities specified above, it was concluded that particle velocity had no affect on charging.

It was found that dielectric particles such as polystyrene could not be charged with an electric field as high as one million volts per meter. Therefore, polystyrene and similar dielectric materials cannot be charged by this method either in the vacuum conditions of space or in a standard atmosphere. Only conducting materials can be charged by impact with a metal plate which has an electric field at its surface.

Three of the seven variables investigated affected charging: electric field, particle size, and particle material. In the next section, these variables will be combined into an empirical formula derived from the observed charging data.

Development of the Charging Formula

From previous discussion, it can be concluded that the particle charge

$$q = q(d^2, \rho_E, E) \tag{5}$$

is a linear function of d^2, E, and an unknown function of resistivity, ρ_E. An exponential function of ρ_E was assumed in order to fit the formula to the observed data. Various powers of ρ_E are shown in Table I.

Table I

Electrical Resistivity Raised to Various Powers

Particle Material	ρ_E (micro ohm cm)	$(\rho_E)^{.11}$	$(\rho_E)^{.12}$	$(\rho_E)^{.13}$
Aluminum	2.66	1.114	1.125	1.136
Zinc	6.0	1.218	1.240	1.262
Tin	11.5	1.308	1.341	1.373
Graphite	1365.0	2.213	2.380	2.555

The formula for q now becomes

$$q = B d^2 (\rho_E)^x E \tag{6}$$

where B is a proportionality constant. Rearrangement gives

$$B = \frac{q}{E d^2 (\rho_E)^x} \tag{7}$$

If measured values of q, known values of E and d, and the values of $(\rho_E)^x$ from Table I are substituted into Eq (7), families of B are found for each value of X. The value giving the most constant B within each family is found to be 0.12. Values of X larger and smaller than those shown in Table I were tried but gave diverging values of B within each family.

The value of B corresponding to $X = .12$ is $B = 8.16 \times 10^{-23}$; thus, the final charging formula is

$$q = 8.16 \times 10^{-23} d^2 (\rho_E)^{.12} E \tag{8}$$

A comparison of measured charges and formula calculated charges is shown in Table II. Of the three variables in Eq (8), the one that most clearly affects q is the electric field, E. This is shown in Figure 3. Variation with surface area (represented by d^2), although based on only one set of data, is plausible because any excess charge on a body tends to reside on its surface. The electrical resistivity raised to the .12 power simply fits Eq (8) to the observed data. The choice of this parameter is not based on any theory and possibly some other parameter of the particle material could be justified theoretically.

Now that a method of predicting particle charge has been developed, an examination of charged particle motion will be made in the next chapter.

Table II

Comparison of Measured and Calculated Charge

Electric Field (volts/meter)	Average Charge per Particle (coulombs x 10^{-12})							
	Aluminum		Zinc		Tin		Graphite	
	Measured	Formula	Measured	Formula	Measured	Formula	Measured	Formula
83300	4.41	4.46	3.00	2.92	1.38	1.38	1.10	1.11
64800	3.15	3.47	2.33	2.26	1.08	1.08	.85	.85
46300	2.18	2.48	1.61	1.62	.74	.77	.61	.62
27800	1.20	1.49	1.00	.97	.46	.46	.27	.37
18520	.84	.99	.67	.65	.31	.31	.19	.25
9260	.45	.50	.28	.32	.14	.15	.08	.12

III. Particle Motion

In Chapter I, motion of charged particles between large spheres was discussed as it applies to the general radiator theory. Possible problem areas associated with this motion are: do the particles rebound from or adhere to the spheres, are collisions elastic or inelastic, is the time of contact between particle and sphere sufficient to heat the particle, will a particle be continuously accelerated throughout several trips so that it may eventually puncture the sphere, and will particles migrate toward one area of a sphere? A simple experiment to demonstrate particle motion between parallel plates is presented in this chapter. High speed motion picture photography is used to study the problems listed above with the parallel plate configuration.

Oscillatory particle motion is verified both in vacuo and at atmospheric pressure in a normal gravity environment, and at atmospheric pressure in a zero gravity environment. The motion pictures show that collisions between particle and plate (both aluminum) are inelastic and therefore, the acceleration on the particle is not cumulative over several trips. A random pattern of particle rebounds after contacting a plate indicates that migration of particles towards one area of a sphere may not be a problem. The particles used are smooth, but irregular in shape. Time of contact and time of flight measurements are made from the motion picture film. The charging formula is verified by use of the flight time and the known electric field between the plates.

Description of Particle Motion Apparatus

Figure 4 shows the chamber (B) that was designed to study charged particle motion. Two aluminum plates were separated by a thin glass cylinder as is shown. The upper plate was connected to a direct current voltage source, while the lower plate was grounded to provide an electric field between the plates. The separation distance was 0.025 meters. Various voltage sources were used; the one shown at (A) in Figure 4 is a small electrostatic generator.

Results

A few particles of various weights were placed on the bottom plate, and voltage applied. According to the theory of equipotential surfaces (assuming an absolutely flat plate and spherical particles) no particle should leave the plate. However, irregularities in particle shape and lack of an ideally smooth plate caused particles to leave the plate as they charged. As voltage was increased, the lightest weight particles began to leave first until all particles had left the bottom plate. Vibration of the support stand caused particles to leave the plate at a lower voltage than without vibration. Vibration aided the particle in escaping the influence of the equipotential surface.

Oscillatory motion was obtained at both 14.7 psia and 1×10^{-6} mm Hg. This was expected since it was shown in Chapter II that air pressure has a very small effect on particle charging. The terminal velocity of a particle falling in a viscous medium can be calculated from Stokes Law. For an aluminum particle weighing 0.9 milligram, the terminal velocity in air is 13.85 meters per second. The maximum velocity attained by this

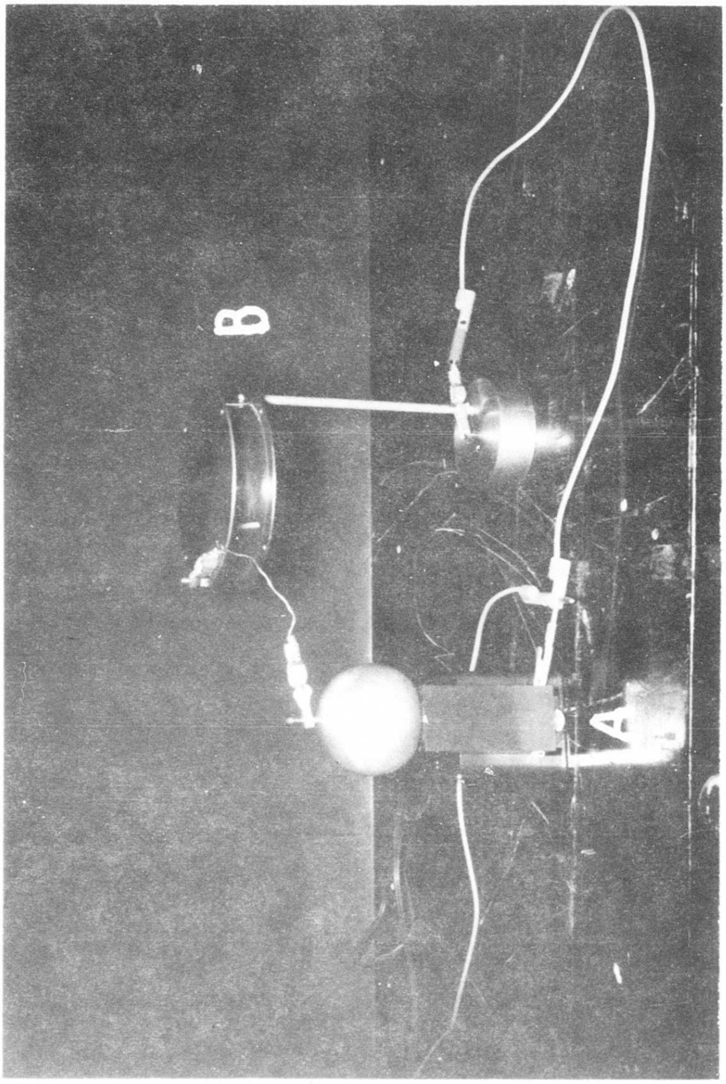

Figure 4

ELECTROSTATIC GENERATOR AND PARTICLE CHAMBER particle on a downward trip of 0.025 meters with E = 528000 volts per meter is calculated to be 1.24 meters per second. Thus the motion results obtained at 14.7 psia are assumed to be valid in vacuum conditions.

The oscillation experiment was performed in the C-131 zero gravity aircraft which is capable of attaining near zero gravity for periods up to 20 seconds. Oscillation occured at zero gravity with no unexpected difference from normal gravity conditions.

Photographing Particle Motion

Detailed study of particle motion with the unaided eye was impractical; therefore, a high speed motion picture camera was employed to effectively reduce the velocity of the particles. A Beckman and Whitley Magnifax High Speed Motion Picture Camera with 63 mm lens was used. Figure 5 shows the photographic apparatus with camera removed. The camera mount is shown at (E). A direct current power supply (D), capable of producing 25000 volts, provided the electric field. Rigidly clamped to the board at (C) is the particle chamber. (A) and (B) are the reflector and lights respectively.

Attached to this thesis is a 200 foot reel of 16 mm film showing particle motion under various electric fields, air pressures, and gravity levels. The following table lists the operating conditions for each of the four film sections:

Table III

Operating Conditions for Each Film Section

Section	Electric Field (volts/meter)	Air Pressure	Gravity	Film Speed (frames/sec)
1	720,000	14.7 psia	one g	2,000
2	600,000	1×10^{-6} mm Hg	one g	2,000
3	60,000	14.7 psia	zero g	800
4	528,000	14.7 psia	zero g	800

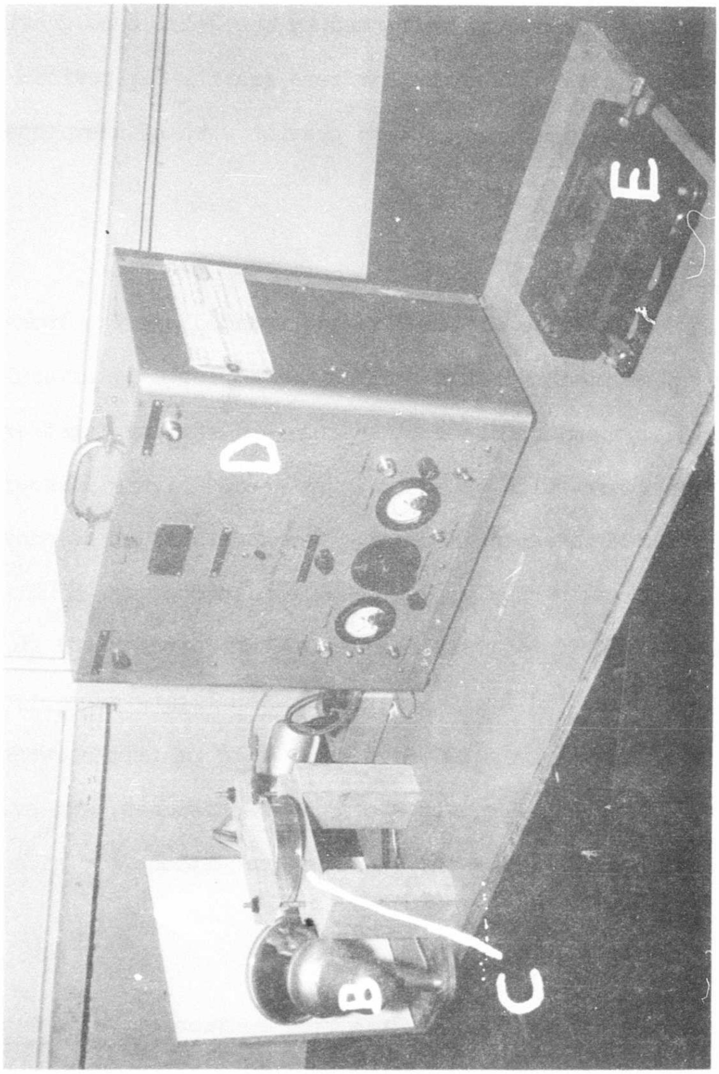

Figure 5

APPARATUS FOR PHOTOGRAPHING PARTICLE MOTION

Two aluminum plates were used in the chamber shown at (C) in Figure 5. All particles shown in the film are aluminum: those in sections 1 and 2 have various weights with an average weight of 0.8 milligrams, while those in sections 3 and 4 weigh 0.9 ± .05 milligrams.

Contact Time

A maximum speed run with the Magnifax camera was made at 3,000 frames per second to measure the time, t_c, that a particle is in contact with a plate. Every second, 120 time ticks were recorded along the edge of the film, thus it was possible to convert the number of frames into time. Other conditions for this run were: pressure, 14.7 psia; electric field, 480,000 volts per meter; particles, aluminum; particle weight, 0.9 ± .05 milligrams; gravity level, one g.

The number of frames that a particle remained in contact was recorded for several contacts. Each of these was converted to time and then averaged. The result was $t_{c\,ave} = 0.9$ milliseconds, a value which will be used in time to heat calculations in the next chapter.

Verification of Charging Formula

Several measurements of flight time, t_f, between plates of the particle chamber were made from section four of the motion picture film. It should be recalled that this section of film was made at zero g with $E = 528{,}000$ volts per meter. The average time to travel the 0.025 meters for six different particles was 0.05 seconds (time for four of the particles was 0.05 seconds).

The average charge on these particles will now be calculated by use of t_f and other known values. The equation for uniformly accelerated motion is

$$D = \frac{1}{2} a t_f^2 \qquad (9)$$

where a is acceleration and t_f is the time of flight. When rearranged Eq (9) can be expressed as

$$a = \frac{2D}{t_f^2} \qquad (10)$$

Another expression for a can be found from

$$Force = Eq = ma \qquad (11)$$

which gives

$$a = \frac{Eq}{m} \qquad (12)$$

These two expressions for a can be equated since they are the same acceleration. The resulting expression for q is then

$$q = \frac{2Dm}{E t_f^2} \qquad (13)$$

Substitution of numbers yields

$$q = \frac{2(.025)(.9 \times 10^{-6})}{528{,}000\,(.05)^2} = 34.1 \times 10^{-12} \text{ coul}$$

It can be shown that a 0.9 milligram aluminum particle is equivalent to a spherical particle 858 microns in diameter. The solution of Eq (8) then gives

$$q = 8.16 \times 10^{-23}(858)^2(1.1245)(528{,}000)$$
$$= 35.7 \times 10^{-12} \text{ coul}$$

The charging formula was derived from data obtained with a maximum E of 83,300 volts per meter. However, it has been used to successfully predict the charge on a particle resulting from an electric field of 528,000 volts per meter. The application of the charging formula in the radiator design will be shown in Chapter IV.

IV. Particle Radiator Design Theory

A general radiator design theory, based upon both experimental and theoretical results, is developed in this chapter. Equations for the following design parameters are determined: electrode geometry, separation distance of the electrodes, number of particles required, electrical power requirements, and total weight.

Particle Motion

It is necessary to assume a typical particle path in order to determine an order of magnitude time of flight between electrode-spheres. The precise solution to particle motion between spheres is extremely complicated and is not justified at this stage of investigation. An order of magnitude time of flight will permit the approximate calculations of the electrical power required, the number of particles required, and the total weight of the radiator.

A typical particle path was presented (see Figure 6) by Smetana: "A representative curvilinear path, ABC, was assumed and replaced by an equal length rectilinear path, AB'C, along which a constant acceleration was to act. The dashed line in Figure 6 represents the curvilinear path for which the time of flight of a typical particle was calculated. Its length is $\frac{\pi}{2}D$" (Ref 2:8) where D is the separation distance between the electrodes.

"The average velocity along each half of the straight line was computed initially; the total time of flight was obtained by adding the time increments required for the particle to travel from A to B and from B to C. When any particle of mass (m) and charge (q) is accelerated from rest

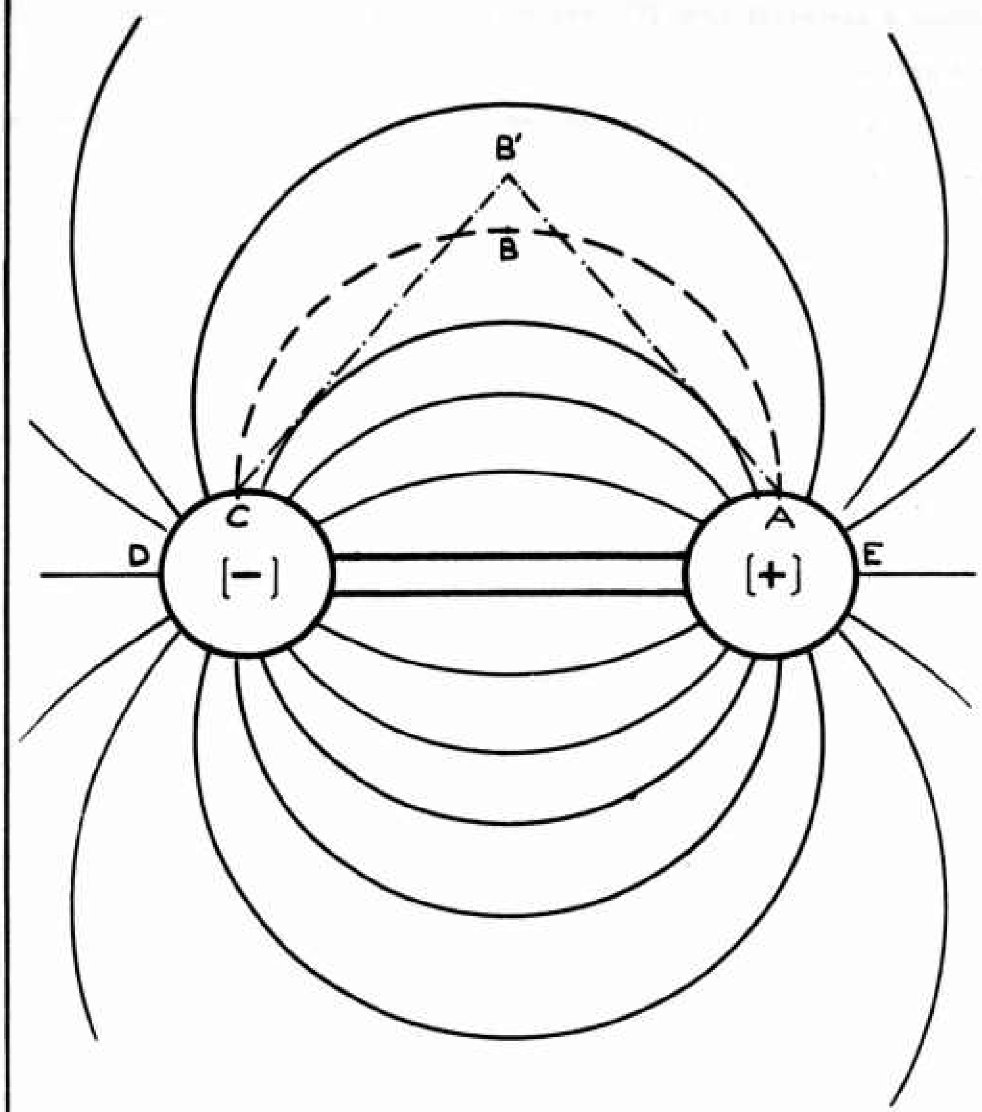

FIGURE 6. System Lines of Force (Ref 2:8)

through a potential drop (V), its velocity (v) can be found from $v^2 = 2qV/m$.

For a particle initially at rest and acted upon by a constant voltage, the velocity of the particle at B is

$$V_B = \left[\frac{qV}{m}\right]^{\frac{1}{2}} \qquad (14)$$

where q is the charge on the particle, V is the potential difference between the two spheres, and m is the mass of the particle. For a particle at B with initial velocity V_B, the velocity of C can be obtained from

$$V_C^2 = V_B^2 + \frac{qV}{m} = 2\,V_B^2 \qquad (15)$$

An approximate time of flight for a single representative particle is therefore obtained from " (Ref 2:9)

$$t_f = \frac{\frac{\pi}{4} D}{\frac{1}{2} V_B} + \frac{\frac{\pi}{4} D}{\frac{1}{2}[V_B + V_C]} = 2.21\left[\frac{m}{qV}\right]^{\frac{1}{2}} D \qquad (16)$$

Heat Transfer

The heat transfer process is dependent on the working fluid supplying excess heat to the sphere and the particles removing heat by conduction and then radiating it into space during their flights between the spheres. For maximum efficiency, it is necessary that the particles depart the heated sphere at the same temperature as that of the sphere. It is therefore necessary that the particles be in contact with the heated sphere for sufficient time to heat up to sphere temperature. Neef developed an approximate expression to find the time to heat. The first approximation was made by assuming a cube containing the same volume as that of a spherical particle; i.e., the side of the cube was 1.612 times the radius of the sphere. Then the average rate of heat transfer is

$$\dot{q} = K_p A_c \frac{\Delta T}{\Delta S} \tag{17}$$

where K_p is the thermal conductivity of the particle, A_c is the area of contact, $\frac{\Delta T}{\Delta S}$ is the change of temperature per change of thickness. When the particles arrive at the heated sphere, they are at a temperature T_A. The rate of heat transfer will be maximum at this time and will decrease exponentially as the temperature of the particle approaches the temperature of the heated sphere, T_1. By selecting a time such that the top of the cube is at T_A and the bottom of the cube is at T_1, a representative rate of heat transfer is obtained. Therefore, the time to heat is given by

$$t_h = \frac{m_p c_p (T_1 - T_A)}{\dot{q}} \tag{18}$$

where m_p is the mass of the particle and c_p is the specific heat of the particle. Substituting Eq (17) into Eq (18) gives

$$t_h = \frac{2.6 \rho_p c_p r^2}{K_p} \tag{19}$$

where ρ_p is the density of the particle material and r is the radius of the particle (Ref 1:17).

Since the maximum time to heat has to be the time of contact between the particle and sphere, Eq (19) is solved for the maximum particle diameter that will heat up to sphere temperature. The equation for maximum particle diameter, in microns, is

$$d = \left[\frac{t_c K_p}{10.4 \rho_p c_p}\right]^{\frac{1}{2}} \times 10^{-6} \tag{20}$$

where t_c is the time of contact between the particle and the heated electrode which can be measured by high speed photography.

Neef determined by use of the Stephan Boltzmann law for radiation that the temperature of the particle arriving at the heated sphere is (Ref 1:18)

$$T_A = \left[\frac{T_1^3 m c_p}{3 T_1^3 A_p e \sigma t_f + m c_p}\right]^{\frac{1}{3}} \tag{21}$$

where T_1 = temperature of the particle as it leaves the heated sphere

A_p = surface area of the particle

e = hemispherical emissivity of the particle

σ = Stephan Boltzmann constant

With T_1 and T_A known, the heat loss rate of a particle can be found from (Ref 2:12)

$$\dot{q} = m c_p \frac{\Delta T}{\Delta t} = \frac{m c_p (T_1 - T_A)}{2 t_f} \tag{22}$$

If $\dot{Q}$ is the total heat rejection rate, then the weight of the particles is given by

$$W_p = m \frac{\dot{Q}}{\dot{q}} \tag{23}$$

The specific weight of the particles in kilograms per kilowatt is obtained by substituting Eq (22) into Eq (23) which gives

$$\frac{W_p}{\dot{Q}} = \frac{2 t_f}{c_p (T_1 - T_A)} \tag{24}$$

Additional heat is generated in the system because of the dissipation of the particles' kinetic energy on impact with the spheres. This requires additional particles for the removal of the added heat. The kinetic energy of a particle is given by

$$(KE)_p = \frac{1}{2} m v_c^2 \tag{25}$$

Substituting Eqs (5) and (6) into Eq (14) gives

$$(KE)_p = q V \tag{26}$$

The total kinetic energy of the particles is

$$KE = N_p q V = \frac{W_p}{m} q V \tag{27}$$

The rate of heat generated by the kinetic energy dissipation is then given by

$$\dot{Q}_{KE} = \frac{W_p q V}{t_f m} \tag{28}$$

Multiplying Eq (28) by Eq (24) gives the additional particle weight required to dissipate the heat caused by kinetic energy effects:

$$W_{P(KE)} = \left[\frac{2 t_f}{c_p (T_1 - T_A)}\right]\left[\frac{W_p q V}{t_f m}\right] \tag{29}$$

and

$$\frac{W_{P(KE)}}{\dot{Q}} = \left[\frac{2 t_f}{c_p (T_1 - T_A)}\right]\left[\frac{W_p}{\dot{Q}} \frac{q V}{t_f m}\right] \tag{30}$$

The specific weight of the particles required is obtained by adding the right hand side of Eq (30) to the right hand side of Eq (24) and solving for $\frac{W_p}{\dot{Q}}$ which gives

$$\frac{W_p}{\dot{Q}} = \frac{\frac{2t_f}{c_p(T_1 - T_A)}}{1 - \left[\frac{2t_f}{c_p(T_1 - T_A)}\right]\left[\frac{qV}{t_f m}\right]} \tag{31}$$

The separation distance between the electrodes is a function of the total surface area of the particles. It is assumed in this study that the effective radiation area of the particles cannot be greater than the area of a sphere which has a diameter equal to the separation distance between the electrodes. If the particles are confined to a smaller volume, then the effective radiation area of the radiator would be less than the surface area of the particles because of radiation interference between particles. Therefore, the minimum separation distance must generate a sphere equal in surface area to the surface area of the particles. Equating the two areas gives

$$\pi D_m^2 = N_p \pi d^2 \times 10^{-12} \tag{32}$$

Substituting $N_p = \frac{W_p}{m}$ into Eq (32) and solving for D_m gives

$$D_m = \left[\frac{W_p}{m}\right]^{\frac{1}{2}} d \times 10^{-6} \tag{33}$$

where D_m is the minimum separation distance, in meters, between electrodes and d is the particle diameter in microns.

It can be seen from Eqs (16), (21), and (31) that the weight of the particles increases as the separation distance is increased. Therefore, for minimum weight operation, Eq (33) must be satisfied. It is important to note that W_p is a function of the time of flight, the time of flight is a function of the separation distance, and the minimum separation distance is a function of W_p, therefore, an iterative solution is required to determine the minimum separation distance.

The weight analysis theory of the two electrode-spheres was developed by Smetana (Ref 2:12). The weight of the spheres is a function of the surface area of the heated sphere and the thickness necessary for meteroriod protection. Smetana used a 95 percent probability of no puncture by meteroriods in a one year period. "The heat-transfer electrode was considered to be a hollow molybdenum sphere in which an oblate sphere of smaller mean radius was fixed. The cross section area along the flow direction was assumed constant. Liquid sodium was arbitrarily selected as the working fluid to flow between the spheres.

Preliminary calculations showed that the electrode surface area will be determined by the area required for heat transfer from within. An approximation was used to determine the heat-transfer coefficient for the sodium flow. Since the mean separation between the inner surface of the outer sphere and the outer surface of the inner sphere was small with respect to the radius of the radius of the electrode, a parallel plate assumption for heat flow was used. Such a correlation for liquid metal flow between parallel plates with heat flowing through only one plate is given by

Brooks (Ref 1:278). The equation is

$$\frac{2hd'}{K_N} = 5.8 + .02\left[\frac{2d'c_N G}{K_N}\right]^{.8} \tag{34}$$

where h = heat transfer coefficient

K_N = thermal conductivity of liquid sodium

d' = mean separation distance between inner and outer sphere

C_N = specific heat of liquid sodium

G = weight flow rate per unit area

The overall coefficient of heat transfer, U, is calculated from the following equation

$$\frac{1}{U} = \frac{1}{h} + \frac{t}{K_m} \tag{35}$$

where t is the thickness of the outer sphere and K_m is the thermal conductivity of molybdenum. The required heat-transfer area, A, is given by

$$A = \frac{\dot{Q}}{U \Delta T} \tag{36}$$

where ΔT is the temperature difference between the bulk temperature of the working fluid and the outer surface of the heated electrode.

Only the outer surface of this electrode must be protected from meteroroid damage. Since very little data is available on meteroroid penetration into molybdenum, that given by Ross et al for steel was used (Ref 9:58). This choice is within the range of assumptions necessary in this study and should be on the conservative side in estimating the thickness required for meteoroid protection at different heat rejection rates.

To obtain minimum weight for the heat rejection sphere, the thickness which was assumed in the calculations of the rejection area was correlated with the minimum thickness required to meet the assumed criteria of the design" (Ref 2:13). The total weight of the two spheres is assumed to be 1.5 times the weight of the outer heated sphere alone. The weight of the spheres is then given by

$$W_s = 1.5\, A\, t\, \rho_m = \frac{1.5 \rho_m \dot{Q} t}{U \Delta T} \qquad (37)$$

where ρ_m is the density of molybdenum. The weight of the connecting structure was arbitrarily chosen to be one kilogram per meter.

Radiator Electrical System

The electrical system for the radiator was described by Smetana: "An electrostatic generator is proposed to provide the electric field that charges the particles and forces them through space. Adequate voltage for electrostatic generators in the range from 200 kilovolts to one megavolt are now in development. A direct current, variable capacitance, dc-excited, machine has been chosen as the most attractive; it is described by Denjelm et al (Ref 3:14). Its ceramic and metal construction lends itself to designs for high temperatures, and except for the flexibility of the stator and rotor disks, the generator is sturdy and reliable. Such electrostatic generators can be designed with a specific mass of .9 kilograms per kilowatt, but Gale estimates this figure can be reduced to .2" (Ref 2:15).

A single particle transfers a positive charge, +q, from the positive electrode to the negative electrode and transfers a negative charge, -q, from the negative electrode to the positive electrode. Since the time of contact is neglegible with respect to the time of flight, the current produced by this charge transfer can be obtained from

$$I = N_P \frac{q}{t_f} = \frac{W_P}{m} \frac{q}{t_f} \tag{38}$$

By use of a specific weight of .9 kilograms per kilowatt, the weight of the electrical system, W_E, can be obtained from

$$W_E = .9\, V I \times 10^{-3} \tag{39}$$

Substituting Eq (38) into Eq (39) gives

$$W_E = .9\, W_P \frac{Vq}{t_f m} \times 10^{-3} \tag{40}$$

or

$$\frac{W_E}{\dot{Q}} = 9 \times 10^{-4} \frac{W_P}{\dot{Q}} \frac{Vq}{t_f m} \tag{41}$$

where $\frac{W_E}{\dot{Q}}$ is the specific weight of the electrical system in kilograms per kilowatt of heat energy to be rejected and q is the charge per particle which is obtained from

$$q = 8.16 \times 10^{-23} d^2 (\rho_E)^{.12} E \tag{8}$$

Substituting $E = \frac{V}{R}$ into Eq (8) gives

$$q = 8.16 \times 10^{-23} d^2 (\rho_E)^{.12} \frac{V}{R} \tag{42}$$

where ρ_E is the resistivity of the particle material and R is the radius of the electrode-sphere.

Limitations to the Theory

There is a high probability that particles will be lost during the operation of the radiator, which will require an additional supply of particles. Particles may be lost from the system because of the collisions of oppositely charged particles resulting in neutralization; however, the probability of complete neutralization is remote. At this stage of design, it is not possible to estimate the number of particles that will be lost because of neutralization effects.

Another potential source of particle loss is the particles that depart the outer tips of the spheres (points D and E in Figure 6) with only a radial velocity component. These particles will depart the field of influence and will not be able to return. A possible device to prevent this loss is an insulated deflector placed on the outer tips to preclude the particles from reaching points D and E in Figure 6. Another possible solution is to use electric field shaping techniques to confine the particles to the desired areas of the electrode-spheres. However, no definite solution can be determined until a more thorough study of particle motion between spheres is completed.

Summary of Equations

Particle Mass

$$m = 5.23 \times 10^{-19} d^3 \rho_P \tag{43}$$

Particle Charge

$$q = 8.16 \times 10^{-23} d^2 (\rho_E)^{.12} \frac{V}{R} \tag{42}$$

Time of Flight

$$t_f = 2.21 \left[\frac{m}{qV}\right]^{\frac{1}{2}} D \tag{16}$$

Arrival Temperature of Particles

$$T_A = \left[\frac{T_1^3 m c_p}{3T_1^3 A_p e \sigma t_f + m c_p}\right]^{\frac{1}{3}} \tag{21}$$

Specific Weight of Particles

$$\frac{W_p}{\dot{Q}} = \frac{\dfrac{2t_f}{c_p(T_1 - T_A)}}{1 - \left[\dfrac{2t_f}{c_p(T_1 - T_A)}\right]\left[\dfrac{qV}{m t_f}\right]} \tag{31}$$

Minimum Separation Distance

$$D_m = \left[\frac{W_p}{m}\right]^{\frac{1}{2}} d \times 10^{-6} \tag{33}$$

Specific Weight of Electrical System

$$\frac{W_E}{\dot{Q}} = 9 \times 10^{-4} \left[\frac{W_p}{\dot{Q}}\right] \frac{Vq}{t_f m} \tag{41}$$

Heat Transfer Coefficient

$$h = \frac{K_N}{2d'} \left[5.8 + .02\left(\frac{2d' c_N G}{K_N}\right)^{.8}\right] \tag{34}$$

Overall Heat Transfer Coefficient

$$\frac{1}{U} = \frac{1}{h} + \frac{t}{K_m} \tag{35}$$

Specific Weight of Electrode-spheres

$$\frac{W_s}{Q} = \frac{1.5\rho_m t}{U \Delta T} \times 10^3 \tag{37}$$

V. Radiator Weight and System Analysis

The particle radiator is proposed for use in a space environment; therefore, the following analysis is based upon minimum weight per kilowatt of heat energy rejected.

The radiator's total specific weight consists of the following elements:

$$\frac{W_T}{\dot{Q}} = \frac{W_P}{\dot{Q}} + \frac{W_E}{\dot{Q}} + \frac{W_S}{\dot{Q}} \qquad (44)$$

where Eqs (31), (37), and (41) are used to find the contributions of each element. The total specific weight is primarily a function of the particle diameter, the operating voltage, the heat rejection temperature, the radiator capacity, and the physical properties of the materials used for the electrode-spheres and particles. For this study, molybdenum was selected as the material for the electrode-sphere because of molybdenum's strength and favorable thermal conductivity at high temperatures. Titanium particles were selected because of titanium's high melting point, low weight, and total hemispherical emissivity of 0.54 (Ref 4:32).

For purposes of analysis, three radiator capacities were arbitrarily selected: five, 10, and 20 megawatts. The weight and dimensions of the electrode-spheres were calculated, for each capacity, from Eqs (34), (35), and (37); these calculations are shown in Appendix A. A heat rejection temperature, T_1, of 950°K was selected as a representative value for purposes of analysis.

To aid in the analysis, an IBM 1620 Digital Computer was used. The computer program incorporating the equations developed in Chapter IV and the corresponding data are presented in Appendix C. $\frac{W_S}{\dot{Q}}$, being a constant for all radiator capacities, was used as an input constant. Incremental particle diameters and operating voltages were used as variable inputs into the computer analysis. For each combination of particle diameter and operating voltage, a minimum separation distance was calculated by an iteration process, thus satisfying Eq (33). Once the minimum separation distance was found, then $\frac{W_P}{\dot{Q}}$, $\frac{W_S}{\dot{Q}}$, and $\frac{W_T}{\dot{Q}}$ were calculated by use of Eqs (31), (41), and (44). The primary outputs of the computer analysis are D_m, $\frac{W_P}{\dot{Q}}$, $\frac{W_S}{\dot{Q}}$, and $\frac{W_T}{\dot{Q}}$.

The conclusions derived from the computer analysis are only as good ad the assumptions made. The assumptions made concerning heat transfer and particle motion are crude, but should be of the right order of magnitude to establish the trends that are shown in Figures 7, 8, 9, and 10 and discussed in the following paragraphs.

Optimum Separation Distance

For each combination of particle size, operating voltage, and radiator capacity, there exists a minimum separation distance. This minimum separation distance is the optimum separation distance which was explained in Chapter IV. Figure 7 is a plot of minimum separation distance versus particle diameter for a 10 megawatt capacity and for various operating voltages. As the particle size is increased, it can be seen from Figure 7 that the minimum separation distance decreases. The slopes of the curves are large between 5 and 30 microns and become significantly smaller between 30 and 50 microns. As the operating voltage was increased, a broader minimum is obtained and less variation in separation distance is evident. Figure 8

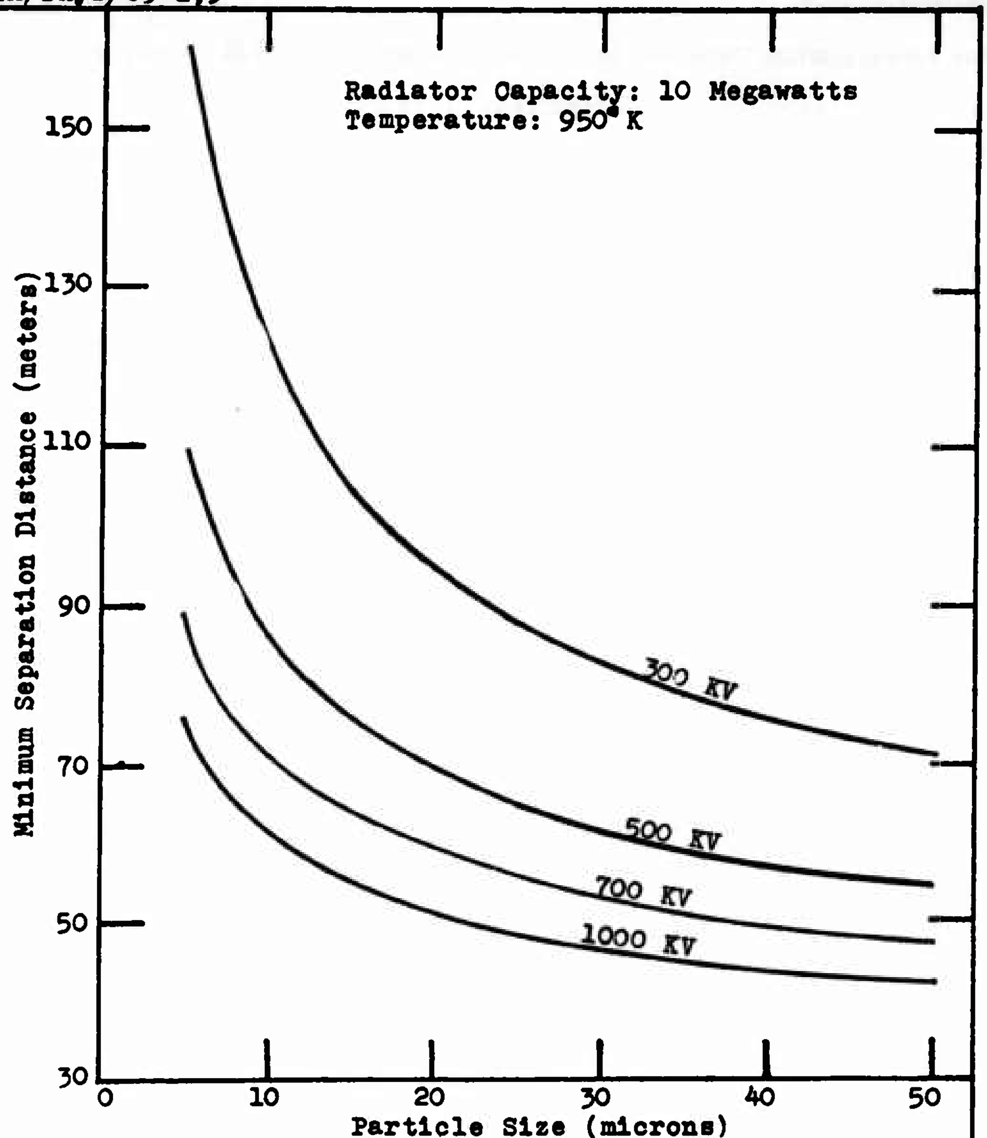

Figure 7

MINIMUM SEPARATION DISTANCE
vs
PARTICLE SIZE

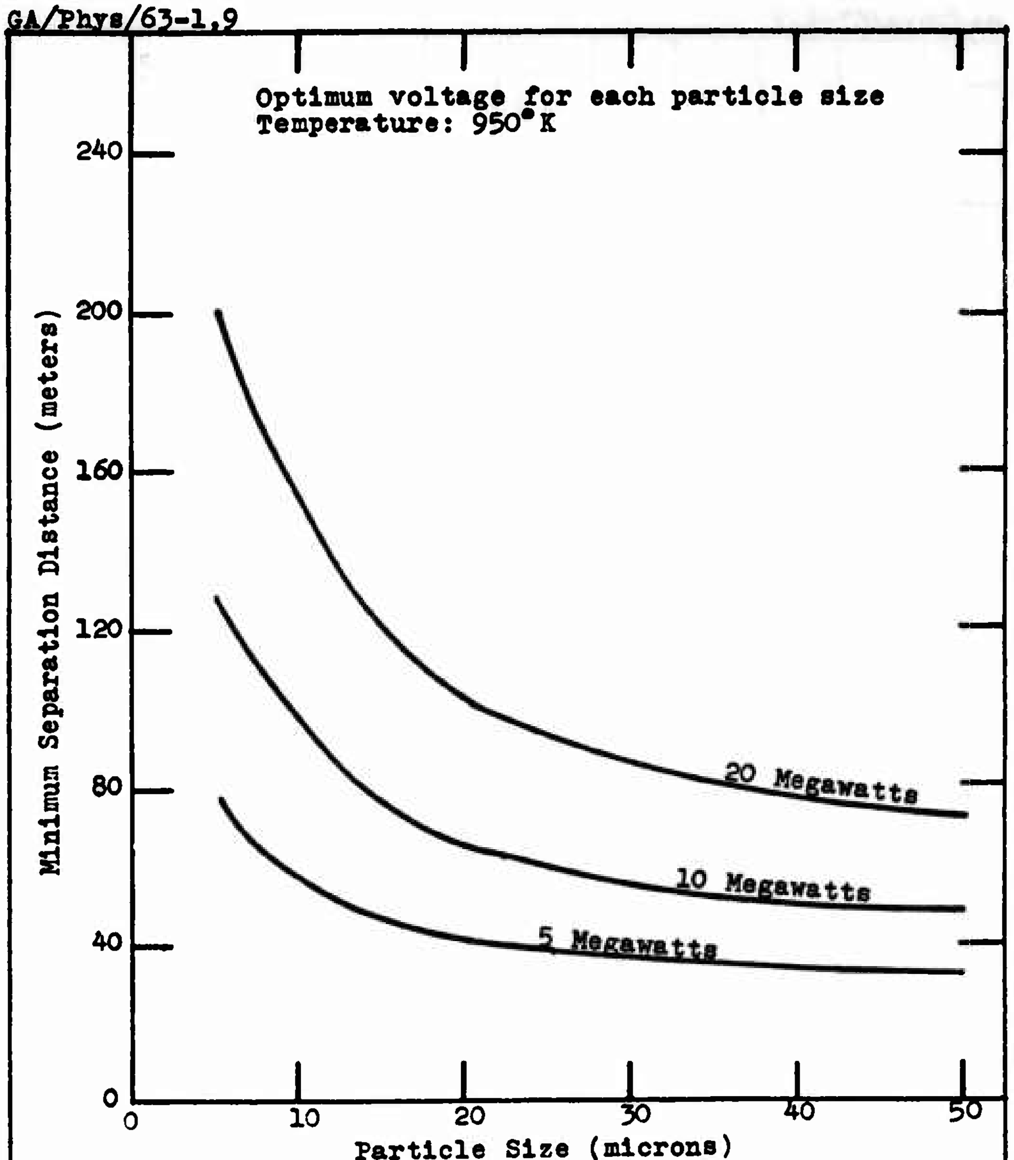

Figure 8

MINIMUM SEPARATION DISTANCE
vs
PARTICLE SIZE

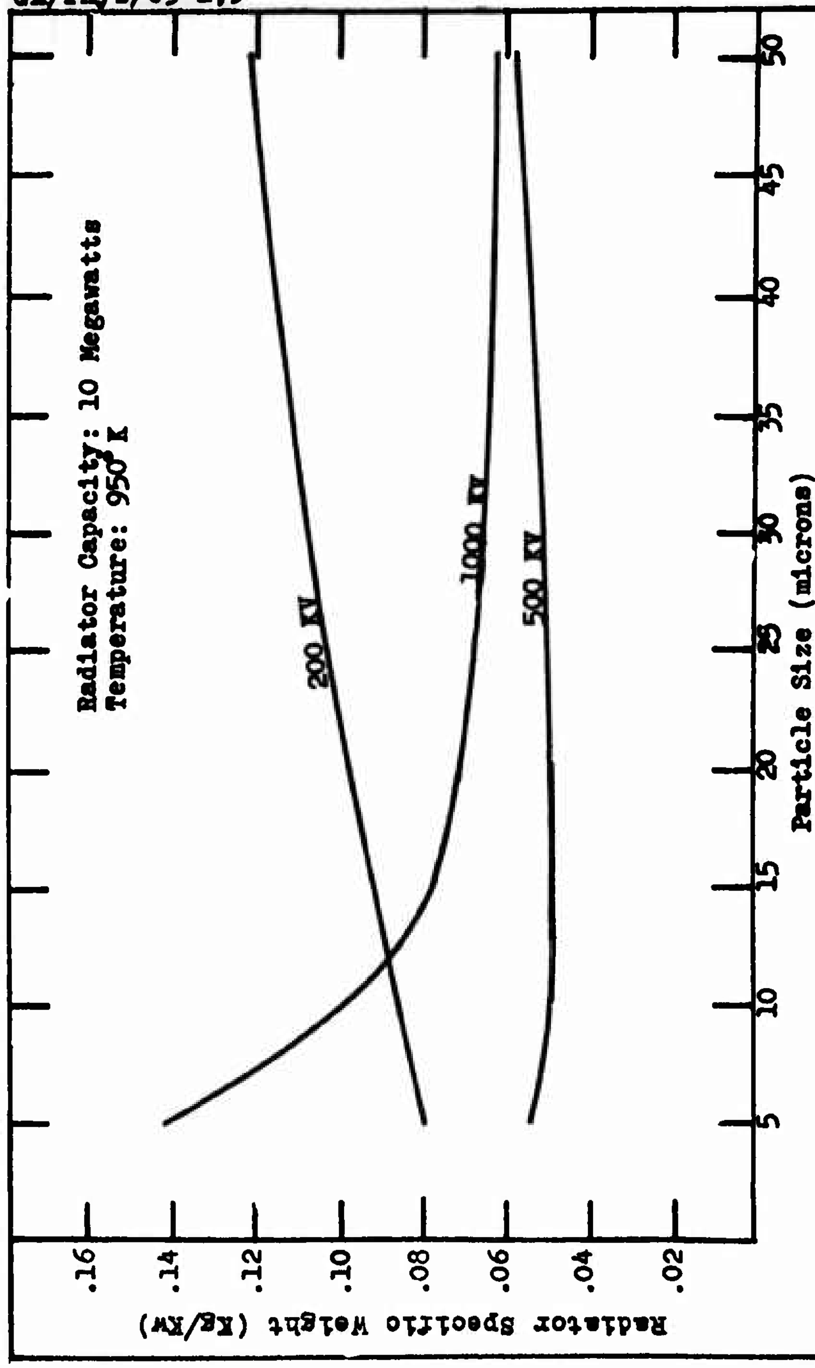

Figure 9

RADIATOR SPECIFIC WEIGHT
vs
PARTICLE SIZE

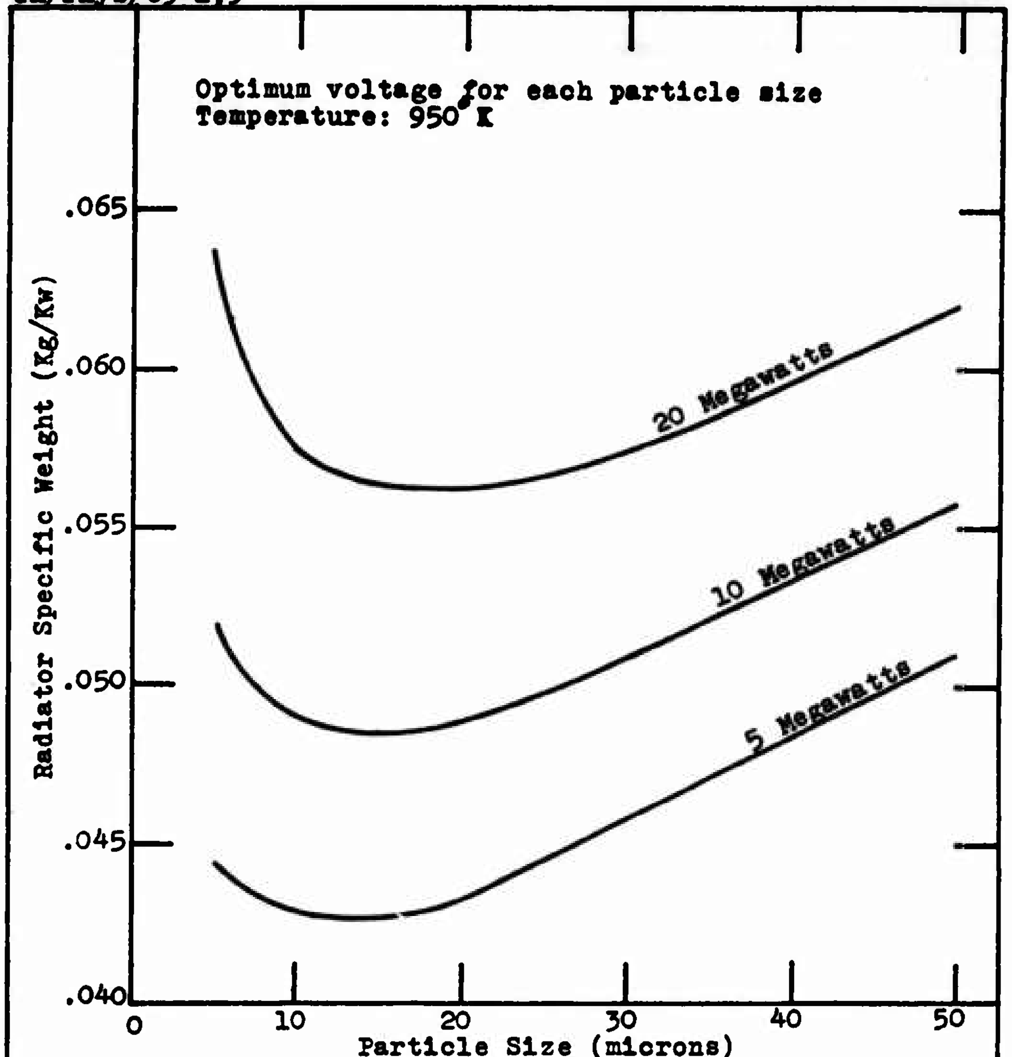

Figure 10

RADIATOR SPECIFIC WEIGHT
vs
PARTICLE SIZE

shows another plot of minimum separation distance versus particle size for the different capacities and optimum voltage for each particle size. It can be seen from Figure 8 that the minimum separation distance increases as the radiator capacity is increased. The increase in minimum separation distance is approximately proportional to the increase in radiator capacity raised to the 0.75 power.

Optimum Particle Size and Operating Voltage

The maximum diameter of titanium particles that would heat up to heat rejection temperature was found to be 91 microns by the solution of Eq (20) and the use of the contact time found in Chapter II. Particle diameters from 5 to 50 microns in increments of 5 microns were selected for purposes of analysis, which allowed a conservative margin for the assumptions made by Neef (Ref 1:17).

Figure 9 shows a plot of radiator specific weight versus particle size for a radiator capacity of 10 megawatts and for various operating voltages. It can be seen from Figure 9 that for each operating voltage there exists a particle size that will minimize the total specific weight. For each particle size, there is an operating voltage that will also minimize the total specifie weight. From the computer data presented in Appendix C, it is seen that as the particle size increased, $\frac{W_P}{Q}$ increased and $\frac{W_E}{Q}$ decreased. These trends are caused by the surface area to mass ratio of the particles. As the particle diameter is increased, its surface area to mass ratio is decreased, and for purposes of radiation heat transfer, a large surface area to mass ratio is desirable for minimum weight. Since the charge carried by the particle is proportional to the surface area of the particle, particles with large surface area to mass ratios will also have large charge to mass ratios, which results in a short time of flight and a large transfer of charge. Therefore, particles with relatively small diameters will give a correspondingly high value of $\frac{W_E}{Q}$.

There exists a complicated tradeoff between particle size and operating voltage which will minimize the sum of $\frac{W_P}{Q}$ and $\frac{W_E}{Q}$, therefore minimizing $\frac{W_T}{Q}$. Figure 10 shows a plot of total specific weight versus particle diameter for the different radiator capacities and optimum voltage for each particle size. It can be seen from Figure 10 and the computer data presented in Appendix C that there exists a particular operating voltage and particle size that will minimize the total specific weight.

Optimization Results

The 20 megawatt radiator was selected as a typical model with which to show the results of the optimization analysis. Once the capacity and the heat rejection temperature were specified, then the remaining design parameters were calculated to minimize the total weight of the radiator. For the 20 megawatt radiator, the computer data presented in Appendix C furnishes the following values for weight minimization:

d = 20 microns

D = 101 meters

V = 800 kilovolts

$$t_f = 4.56 \text{ seconds}$$

$$R = 0.797 \text{ meters}$$

$$\frac{W_P}{\dot{Q}} = 0.02496$$

$$\frac{W_E}{\dot{Q}} = 0.01177$$

$$\frac{W_S}{\dot{Q}} = 0.01940$$

$$\frac{W_T}{\dot{Q}} = 0.05614$$

From the above data, the weights of the titanium particles and the electrostatic generator were computed to be 499 and 250 kilograms respectively. The weight of the electrode-spheres and connecting structure was computed to be 1223 kilograms.

The optimization results of the 5 and 10 megawatt capacities are shown in Table IV in which a comparison of the particle radiator is made with the standard tube-and-header radiator. It can be seen from Table IV that the particle radiator concept has a marked weight advantage over the conventional radiator. It should be noted that the tube-and-header radiator has been under development a much longer time than the particle radiator and has the advantage of optimization of design and materials. Further refinements in the particle radiator should increase its weight advantage over the conventional radiator. Comparison with a recently suggested belt radiator shows the particle radiator to weigh approximately the same as the belt radiator (Ref 2:35, 36).

Table IV

Typical Radiators

Heat Rejection Rate	5	10	20	mw
Conventional Tube-and-Header Radiator (Ref 2:36)				
Isothermal Radiation Temperature	950	950	950	°K
Required Radiating Area	121	242	485	m^2
Tube Wall Thickness	.635	.635	.635	mm
Weight of Tubes	949	1898	3795	kg
Total Radiator Weight - Steel	1770	3540	7080	kg
Particle Radiator				
Maximum Heat Rejection Temperature	950	950	950	°K
Electrode Separation	60	76	101	m
Radius of Electrodes	.399	.564	.797	m
Operating Voltage	300	500	800	kv
Weight of Particles	88	209	499	kg
Weight of Electrostatic Generator	29	83	235	kg
Weight of Electrodes and Structure	157	270	489	kg
Total Radiator Weight - Molybdenum	274	562	1223	kg

System Considerations

Up to this point in the analysis, only minimization of weight has been considered. However, other considerations are of vital importance to the analysis. A thermal rejection temperature of 950°K was the only temperature considered because of the complexity of the calculations involved. The optimum heat rejection temperature cannot be determined until cycle conditions have been specified. Smetana stated in his study, "Presently the accepted design practice is to reject heat from the power generating equipment at a temperature higher than that giving a maximum power plant efficiency. This increases the weight of the power generating unit but decreases the ponderous radiator weight by allowing heat rejection at a higher temperature. When a particle radiator can be utilized in a system, it will prove beneficial to operate the power plant at somewhat lower heat rejection temperature. A lower T_1 will increase radiator weight but will permit smaller generator and turbine sizes" (Ref 2:31).

System reliability was also discussed by Smetana: "If the reliabilities of the conventional and particle radiator are assumed equal, use of the particle radiator can increase the reliability of the entire power system in at least two ways. Initially, the operating temperatures can be reduced throughout the system, thus allowing simpler and easier construction. Since the particle system can operate very competitively at heat rejection temperatures lower than those essential for conventional radiators, operating temperatures at all stages of the power cycle can be reduced. This reduction in itself will increase system reliability, and furthermore, will permit design consideration for those lower temperatures. For example, refractory alloys which are difficult to fabricate, corrode easily, and react with liquid metals can be replaced by more reliable stainless steels" (Ref 2:31).

VI. Conclusions and Recommendations

As discussed in Chapter I, problem areas that needed experimental investigation were particle charging, heat transfer, and particle motion between spheres. Only particle charging experimentation was accomplished in this study. The results of the charging experimentation presented in Chapters II and III showed that charge transfer does occur and that the charge transferred can be calculated by an empirical formula presented as Eq (8). In addition, the associated oscillatory particle motion was confirmed under simplified conditions, i.e., between parallel plates. Times of contact between particles and parallel plates were measured in order to determine a representative time of contact for use in computer analysis.

The results of the computer analysis, based upon experimental quantities, showed that a total specific weight on the order of .055 kilograms per kilowatt is feasible. The weight advantage of the particle radiator is shown in Table IV. Weight reduction by a factor of 6 over the conventional radiator appears feasible. Further weight reduction of the particle radiator may be possible by design refinements in the internal heat transfer mechanism, connecting structure, and electrostatic generator. Since minimum weight is the primary consideration of the type of radiator to be used in nuclear power plants for future space behicles, the weight advantage of the particle radiator is of paramount importance.

The assumptions made concerning heat transfer and particle motion have not yet been proven experimentally. However, all the assumed conditions were estimated conservatively and the results obtained should have been realistic. Optimization of materials used for the electrode-spheres and particles was not considered in this study. Optimization of these materials will be more appropriate after heat transfer experimentation is completed.

The primary conclusion of this investigation is that the particle radiator concept, offering an appreciable weight advantage, is feasible. Therefore, there is sufficient justification for continued studies toward the ultimate goal of an operational particle radiator.

As discussed earlier, factors such as reliability and cost have not been considered. In view of this and the fact that experimental heat transfer and particle motion data are required, the following design and development studies are recommended to be accomplished before the particle radiator is considered for use in space power systems:

1. An experimental study to determine the heat transferred by conduction from a heated sphere to micron sized particles in vacuo.
2. A study to determine the optimum materials for the electrode-spheres and particles.
3. A theoretical study to determine particle motion between spheres in conjunction with a radiation heat transfer study.
4. Design and development of a prototype particle radiator for use in an orbital environment to investigate system reliability, particle loss, heat transfer efficiency, and overall operation.

Bibliography

1. Neef, C.F. Design of a Dielectric Variable-Area Thermal Radiator. Unpublished thesis. Wright-Patterson Air Force Base, Ohio: Air Force Institute of Technology, August 1961.

2. Smetana, D.W. Design Analysis of a Particle Thermal Radiator for Space Vehicles. Unpublished thesis. Wright-Patterson Air Force Base, Ohio: Air Force Institute of Technology, August 1962.

3. Syracuse University Research Institute. Air Research and Development Command Technical Report 59-66. Air Weapons Materials Application Handbook Metals and Alloys. Wright-Patterson Air Force Base, Ohio: Wright Air Development Center, 1959

4. Wade, W.R. National Advisory Committee for Aeronautics. Technical Note 4206. Total Hemispherical Emissivity of Oxidized Metals. Washington: GPO, 1958

Appendix A

Specific Constants

General

σ	Stephan Boltzmann constant	5.67×10^{-8} joules/meter^2 sec °K^4

Titanium (950 °K)

ρ_p	density	4540 kilograms/meter^3
C_p	specific heat	753 joules/kilogram °K
e	total hemispherical emissivity	0.54 (Ref 4:32)
K_p	thermal conductivity	20.76 joules/meter sec °K

Molybdenum (950 °K)

ρ_m	density	10200 kilograms/meter^3
K_m	thermal conductivity	65 BTU/hour ft °K

Liquid Sodium

C_N	specific heat	0.305 BTU/lb °R
K_N	thermal conductivity	30 BTU/hour ft °R

(Data taken in part from Ref 3)

Appendix B

Sample Calculations of Electrode Specific Weight

Illustrated below are a set of sample calculations which show the method by which the specific weight of the electrodes was calculated for heat rejection rates of five, 10, and 20 megawatts.

__Film coefficient.__ Equation (34) was solved for h :

$$h = \frac{K_N}{2d'}\left[5.8 + .02\left(\frac{2d'c_N G}{K_N}\right)^{.8}\right]$$

where values for d' and G were taken as 0.0328 ft and 1.25 x 10^7 lbs/hr-ft^2 from state of the art designs. Physical property data are given in Appendix A.

$$h = \frac{30}{2(.0328)}\left[5.8 + .02\left(\frac{2(.0328)(.305)1.25\times10^7}{30}\right)^{.8}\right]$$

$$= 14{,}500 \ \text{BTU/hr ft}^2\ {}^\circ\text{R}$$

__Overall heat transfer coefficient.__ Under equilibrium conditions the heat flow rate through the molybdenum is equal to that through the liquid sodium; therefore, U, is found from Equation (35)

$$\frac{1}{U} = \frac{1}{h} + \frac{t}{K_m}$$

A value of 125 mils was selected for the thickness of the molybdenum, therefore

$$\frac{1}{U} = \frac{1}{14{,}500} + \frac{.0104}{65}$$

$$U = 4400\ BTU/hr\ ft^2\ {}^\circ R$$

$$= 25{,}000\ joules/sec\ m^2\ {}^\circ K$$

Electrode specific weight. $\frac{W_s}{\dot{Q}}$ is found from Equation (37)

$$\frac{W_s}{\dot{Q}} = \frac{1.5 \rho_m t}{U \Delta T} \times 10^3$$

where $\Delta T = T_B - T_i$. For this calculation ΔT was assumed to be 100°K.

$$\frac{W_s}{\dot{Q}} = \frac{1.5(1.02 \times 10^4)(.00317)}{25{,}000\ (100)} \times 10^3 = .0194\ Kg/Kw$$

For the five megawatt capacity

$$W_s = .0194\,\dot{Q} = .0194(5 \times 10^3) = 97\ Kg$$

Similarly, W_s for the 10 and 20 megawatt capacities were calculated to be 194 and 388 kilograms respectively.

Electrode-sphere radius. Equation (36) gives the required heat transfer area.

$$A = \frac{\dot{Q}}{U \Delta T}$$

For the five megawatt capacity

$$A = \frac{5 \times 10^6}{25{,}000(100)} = 2\ m^2$$

which gives a corresponding radius of 0.399 meters. Similarly, the radii for the 10 and 20 megawatt capacities were calculated to be 0.564 and 0.797 meters respectively.

(Calculations taken in part from Ref 2:46)

Appendix C

IBM 1620 Computer Data

The printout of the program used on the IBM 1620 Computer together with a list of computer symbols and output data are presented in this Appendix. The computer program is reproduced on page 57. A list of symbols used in the computer program is presented on pages 58 and 59. Page 60 through page 66 contains the data for the 5 megawatt radiator; page 67 through page 73 contains the data for the 10 megawatt radiator; page 74 through page 80 contains the data for the 20 megawatt radiator.

The output data for each radiator is presented in blocks and each block consists of two lines. The first line of each block contains, in the following order, the heat rejection temperature in ^{o}K, the minimum separation distance in meters, and the operating voltage in volts. The second line of each block contains, in the following order, the particle diameter in microns, the specific number of particles in 10^6 per kilowatt, the time of flight in seconds, the specific weight of the particles, the specific weight of the electrical system, and the total specific weight of the radiator. All specific weights have dimensions of kilograms per kilowatt.

IBM 1620 COMPUTER PROGRAM PRINTOUT

```
1     READ,DH,GG,HG,HH,TB,DO,VO,SO,DS,DV,DD,VM,SM,WS,CC,DB
      PUNCH 51,WS,CC,DB
4     V=VO
5     S=SO
6     D=DO
      M=1
8     W=5.236E-19*S*S*S*DH
      Q=8.16E-23*S*S*HG**.12*V/DB
      FT=2.21*D*SQRT(W/(Q*V))
      TA=(DH*TB*TB*TB*S*GG/((.25515*HH*FT*TB*TB*TB)
                 +(S*GG*DH)))**.3333
      WW=FT*2000./((TB-TA)*GG)
      WG=V*Q/(FT*W)
      WP=WW/(1.-(WW*WG*.001))
      PP=WP*1.E-6/W
      DM=S*.001*SQRT(PP*CC)-(2.*DB)+1.
      D=D+DD
      IF(DM-D)9,9,8
9     GO TO(11,19),M
11    D=D-DD
      DD=DD/10.0
      D=D+DD
      M=M+1
12    GO TO 8
19    DW=D-1.0
      DD=DD*10.0
      WE=.0009*WG*WP
      WT=WP+WE+WS
      PUNCH 52,TB,DW,V
      PUNCH 53,S,PP,FT,WP,WE,WT
      S=S+DS
      IF(SM-S)10,6,6
10    V=V+DV
      IF(VM-V)1,5,5
51    FORMAT(///F16.5,F16.0,F16.4)
52    FORMAT(/F6.0,F12.0,F18.0 )
53    FORMAT(F6.0,F10.2,F12.5,F12.5,F12.5,F12.5)
      END
```

List of Computer Symbols

DH - Density of particle material (Kg/m^3).

GG - Specific heat of particle material (joules/m-sec-°K).

HG - Electrical resistivity of particle material (u ohms-cm).

HH - Total hemispherical emissivity of particle material.

TB - Heat rejection temperature (°K).

DO - Initial separation distance (meters)

VO - Initial voltage (volts).

SO - Initial particle diameter (microns).

DS - Increment of particle diameter (microns).

DV - Increment of operating voltage (volts).

DD - Increment of separation distance (meters).

VM - Maximum operating voltage (volts).

SM - Maximum particle diameter (microns).

WS - Specific weight of electrode-spheres (Kg/Kw).

CC - Radiator capacity (Kw).

DB - Radius of electrode-spheres (meters).

W - Weight per particle (Kg).

Q - Charge per particle (coulombs).

FT - Time of flight (secs).

TA - Arrival temperature of particle (°K).

DW - Minimum separation distance (meters).

V - Operating voltage (volts).

S - Particle diameter (microns).

PP - Specific number of particles (10^6/Kw).

WP - Specific weight of particles (Kg/Kw).

WE - Specific weight of electrical system (Kg/Kw).

WT - Total specific weight of radiator (Kg/Kw).

01940 5000. .3985

950.	183.		100000.		
5.	269518.73	23.39018	.08008	.00092	.10040
950.	136.		100000.		
10.	37376.02	24.58309	.08884	.00048	.10873
950.	115.		100000.		
15.	11918.94	25.45898	.09562	.00033	.11536
950.	103.		100000.		
20.	5359.47	26.32993	.10192	.00026	.12158
950.	94.		100000.		
25.	2875.32	26.86553	.10679	.00021	.12641
950.	88.		100000.		
30.	1744.84	27.55122	.11198	.00018	.13157
950.	83.		100000.		
35.	1142.57	28.06788	.11645	.00015	.13601
950.	79.		100000.		
40.	793.44	28.55976	.12071	.00014	.14025
950.	76.		100000.		
45.	578.00	29.14187	.12520	.00012	.14473
950.	73.		100000.		
50.	433.61	29.50566	.12884	.00011	.14836
950.	103.		200000.		
5.	86125.32	6.58248	.02559	.00418	.04917
950.	79.		200000.		
10.	12725.30	7.13994	.03024	.00227	.05192
950.	69.		200000.		
15.	4279.23	7.63769	.03433	.00161	.05534
950.	62.		200000.		
20.	1969.90	7.92454	.03746	.00127	.05813
950.	58.		200000.		
25.	1097.43	8.28830	.04076	.00105	.06122
950.	55.		200000.		
30.	682.88	8.60975	.04382	.00091	.06414

950.	52.		200000.		
35.	454.33	8.79234	.04630	.00080	.06651
950.	50.		200000.		
40.	321.94	9.03790	.04897	.00072	.06910
950.	49.		200000.		
45.	240.31	9.39441	.05205	.00066	.07211
950.	47.		200000.		
50.	182.09	9.49839	.05410	.00061	.07412
950.	77.		300000.		
5.	47873.68	3.28059	.01422	.01050	.04412
950.	60.		300000.		
10.	7372.38	3.61516	.01752	.00586	.04279
950.	53.		300000.		
15.	2552.19	3.91108	.02047	.00422	.04410
950.	49.		300000.		
20.	1220.25	4.17529	.02320	.00336	.04597
950.	46.		300000.		
25.	690.53	4.38232	.02564	.00283	.04788
950.	44.		300000.		
30.	437.18	4.59187	.02805	.00246	.04992
950.	42.		300000.		
35.	295.96	4.73434	.03016	.00220	.05176
950.	41.		300000.		
40.	213.69	4.94071	.03251	.00199	.05390
950.	40.		300000.		
45.	160.16	5.11260	.03469	.00182	.05592
950.	39.		300000.		
50.	123.64	5.25443	.03673	.00169	.05783
950.	64.		400000.		
5.	33011.09	2.04504	.00980	.02064	.04985
950.	51.		400000.		
10.	5289.35	2.30466	.01257	.01174	.04371

950.	45.		400000.		
15.	1860.00	2.49055	.01492	.00859	.04292
950.	42.		400000.		
20.	906.47	2.68411	.01723	.00691	.04355
950.	40.		400000.		
25.	523.28	2.85803	.01943	.00585	.04469
950.	38.		400000.		
30.	332.85	2.97427	.02136	.00515	.04591
950.	37.		400000.		
35.	229.89	3.12804	.02343	.00460	.04743
950.	36.		400000.		
40.	166.71	3.25364	.02536	.00419	.04895
950.	35.		400000.		
45.	125.46	3.35514	.02717	.00387	.05045
950.	35.		400000.		
50.	98.73	3.53663	.02933	.00357	.05230

950.	56.		500000.		
5.	25483.91	1.43153	.00757	.03558	.06255
950.	45.		500000.		
10.	4181.66	1.62682	.00994	.02055	.04989
950.	41.		500000.		
15.	1521.81	1.81533	.01220	.01508	.04668
950.	38.		500000.		
20.	745.67	1.94279	.01418	.01227	.04585
950.	36.		500000.		
25.	432.65	2.05778	.01606	.01050	.04597
950.	35.		500000.		
30.	280.82	2.19157	.01802	.00922	.04664
950.	34.		500000.		
35.	194.77	2.29953	.01985	.00829	.04754
950.	33.		500000.		
40.	141.79	2.38600	.02157	.00760	.04857
950.	33.		500000.		
45.	108.71	2.53074	.02355	.00695	.04990

950.	32.		500000.		
50.	84.53	2.58679	.02511	.00653	.05104
950.	51.		600000.		
5.	21269.13	1.08642	.00631	.05634	.08206
950.	42.		600000.		
10.	3590.05	1.26530	.00853	.03266	.06060
950.	38.		600000.		
15.	1312.81	1.40208	.01053	.02425	.05418
950.	36.		600000.		
20.	656.38	1.53378	.01248	.01970	.05159
950.	34.		600000.		
25.	382.60	1.61955	.01421	.01699	.05060
950.	33.		600000.		
30.	249.28	1.72195	.01600	.01500	.05040
950.	32.		600000.		
35.	173.52	1.80355	.01768	.01356	.05065
950.	32.		600000.		
40.	128.57	1.92808	.01956	.01228	.05124
950.	31.		600000.		
45.	97.41	1.98113	.02110	.01146	.05196
950.	31.		600000.		
50.	77.02	2.08830	.02288	.01061	.05290
950.	48.		700000.		
5.	18817.33	.87644	.00559	.08411	.10910
950.	40.		700000.		
10.	3218.69	1.03290	.00765	.04883	.07588
950.	36.		700000.		
15.	1181.58	1.13853	.00947	.03659	.06547
950.	34.		700000.		
20.	593.06	1.24163	.01127	.02994	.06061
950.	33.		700000.		
25.	352.07	1.34735	.01307	.02559	.05807

950.	32.		700000.		
30.	230.08	1.43123	.01476	.02267	.05684
950.	31.		700000.		
35.	160.61	1.49759	.01636	.02058	.05635
950.	30.		700000.		
40.	117.63	1.54935	.01789	.01903	.05633
950.	30.		700000.		
45.	90.55	1.64333	.01961	.01748	.05650
950.	29.		700000.		
50.	70.79	1.67448	.02103	.01656	.05700
950.	46.		800000.		
5.	17325.59	.73493	.00514	.12062	.14517
950.	38.		800000.		
10.	2951.94	.85860	.00701	.07036	.09678
950.	35.		800000.		
15.	1101.91	.96854	.00884	.05239	.08063
950.	33.		800000.		
20.	554.60	1.05447	.01054	.04305	.07300
950.	32.		800000.		
25.	330.00	1.14321	.01225	.03692	.06858
950.	31.		800000.		
30.	216.16	1.21319	.01387	.03282	.06609
950.	30.		800000.		
35.	151.24	1.26812	.01541	.02990	.06471
950.	30.		800000.		
40.	112.42	1.35568	.01710	.02715	.06366
950.	29.		800000.		
45.	85.57	1.38999	.01853	.02551	.06345
950.	29.		800000.		
50.	67.85	1.46517	.02016	.02369	.06325
950.	45.		900000.		
5.	16545.42	.63907	.00491	.16766	.19197

950.	37.		900000.		
10.	2798.94	.74311	.00665	.09756	.12362
950.	34.		900000.		
15.	1045.08	.83633	.00838	.07283	.10061
950.	32.		900000.		
20.	526.88	.90890	.01001	.06006	.08948
950.	31.		900000.		
25.	313.98	.98443	.01166	.05163	.08270
950.	30.		900000.		
30.	206.03	1.04360	.01322	.04602	.07865
950.	29.		900000.		
35.	144.41	1.08965	.01471	.04205	.07617
950.	29.		900000.		
40.	107.44	1.16488	.01634	.03822	.07397
950.	29.		900000.		
45.	82.85	1.23554	.01794	.03517	.07252
950.	28.		900000.		
50.	65.01	1.25747	.01931	.03348	.07220

950.	45.		1000000.		
5.	16341.22	.57516	.00485	.22715	.25140
950.	36.		1000000.		
10.	2699.12	.65072	.00641	.13265	.15846
950.	33.		1000000.		
15.	1006.14	.73056	.00807	.09910	.12657
950.	32.		1000000.		
20.	513.62	.81801	.00976	.08032	.10948
950.	30.		1000000.		
25.	302.67	.85741	.01124	.07056	.10120
950.	30.		1000000.		
30.	201.06	.93924	.01290	.06161	.09392
950.	29.		1000000.		
35.	141.07	.98068	.01437	.05635	.09013
950.	29.		1000000.		
40.	104.96	1.04839	.01596	.05123	.08660

950.	28.		1000000.		
45.	80.14	1.07364	.01735	.04833	.08509
950.	28.		1000000.		
50.	63.60	1.13172	.01889	.04493	.08323

.01940 10000. .5640

950.	410.		100000.		
5.	676016.09	62.34359	.20087	.00061	.22088
950.	301.		100000.		
10.	91083.01	64.72759	.21651	.00031	.23623
950.	252.		100000.		
15.	28420.89	66.36958	.22801	.00021	.24763
950.	223.		100000.		
20.	12515.08	67.81766	.23800	.00016	.25756
950.	203.		100000.		
25.	6640.60	69.02223	.24665	.00013	.26618
950.	188.		100000.		
30.	3961.42	70.02311	.25425	.00011	.27377
950.	176.		100000.		
35.	2559.41	70.80593	.26085	.00010	.28035
950.	167.		100000.		
40.	1761.63	71.82397	.26801	.00008	.28749
950.	159.		100000.		
45.	1264.71	72.53144	.27395	.00007	.29343
950.	153.		100000.		
50.	945.22	73.56976	.28086	.00007	.30034

950.	223.		200000.		
5.	200799.61	16.95441	.05966	.00267	.08174
950.	167.		200000.		
10.	28227.95	17.95599	.06710	.00142	.08792
950.	142.		200000.		
15.	9092.34	18.69936	.07294	.00098	.09333
950.	127.		200000.		
20.	4100.37	19.31130	.07797	.00076	.09814
950.	117.		200000.		
25.	2225.73	19.89064	.08267	.00063	.10270
950.	110.		200000.		
30.	1359.65	20.48548	.08726	.00053	.10720

950.	104.		200000.		
35.	894.64	20.91993	.09118	.00047	.11105
950.	99.		200000.		
40.	622.93	21.28914	.09477	.00042	.11459
950.	95.		200000.		
45.	453.90	21.66819	.09832	.00038	.11810
950.	92.		200000.		
50.	343.53	22.11901	.10208	.00035	.12183
950.	160.		300000.		
5.	103746.82	8.10973	.03082	.00650	.05673
950.	122.		300000.		
10.	15118.31	8.74503	.03593	.00351	.05885
950.	105.		300000.		
15.	4994.52	9.21799	.04007	.00247	.06194
950.	95.		300000.		
20.	2301.88	9.63031	.04377	.00194	.06511
950.	88.		300000.		
25.	1268.01	9.97365	.04709	.00161	.06811
950.	83.		300000.		
30.	783.47	10.30482	.05028	.00139	.07107
950.	79.		300000.		
35.	522.46	10.59407	.05324	.00122	.07387
950.	76.		300000.		
40.	369.46	10.89545	.05620	.00110	.07671
950.	73.		300000.		
45.	271.24	11.10020	.05875	.00100	.07916
950.	71.		300000.		
50.	207.17	11.38007	.06156	.00092	.08188
950.	129.		400000.		
5.	67349.83	4.90385	.02001	.01241	.05182
950.	100.		400000.		
10.	10120.02	5.37604	.02405	.00680	.05026

950.	87.		400000.		
15.	3415.81	5.72832	.02740	.00485	.05165
950.	79.		400000.		
20.	1595.14	6.00627	.03033	.00384	.05357
950.	74.		400000.		
25.	893.91	6.29020	.03320	.00321	.05581
950.	70.		400000.		
30.	557.69	6.51810	.03579	.00278	.05797
950.	67.		400000.		
35.	375.90	6.73863	.03831	.00247	.06018
950.	65.		400000.		
40.	268.95	6.98885	.04091	.00222	.06254
950.	63.		400000.		
45.	199.79	7.18471	.04327	.00203	.06471
950.	61.		400000.		
50.	152.87	7.33293	.04542	.00188	.06670
950.	110.		500000.		
5.	49204.92	3.34526	.01462	.02077	.05479
950.	86.		500000.		
10.	7551.50	3.69871	.01795	.01153	.04888
950.	76.		500000.		
15.	2608.31	4.00324	.02092	.00828	.04860
950.	69.		500000.		
20.	1229.13	4.19678	.02337	.00661	.04939
950.	65.		500000.		
25.	696.74	4.42014	.02587	.00556	.05084
950.	62.		500000.		
30.	440.03	4.61854	.02824	.00484	.05248
950.	60.		500000.		
35.	300.45	4.82767	.03062	.00430	.05432
950.	58.		500000.		
40.	215.47	4.98897	.03278	.00390	.05608
950.	56.		500000.		
45.	160.41	5.10913	.03474	.00359	.05774

950.	55.		500000.		
50.	124.36	5.28932	.03695	.00332	.05967
950.	98.		600000.		
5.	39020.36	2.48360	.01159	.03195	.06294
950.	77.		600000.		
10.	6080.87	2.75970	.01445	.01792	.05177
950.	68.		600000.		
15.	2119.14	2.98487	.01700	.01299	.04939
950.	63.		600000.		
20.	1020.85	3.19320	.01941	.01040	.04921
950.	60.		600000.		
25.	586.37	3.40011	.02177	.00876	.04994
950.	57.		600000.		
30.	371.30	3.53840	.02383	.00768	.05091
950.	55.		600000.		
35.	254.18	3.68780	.02590	.00686	.05217
950.	53.		600000.		
40.	182.73	3.79907	.02780	.00626	.05346
950.	52.		600000.		
45.	137.87	3.95349	.02986	.00574	.05501
950.	51.		600000.		
50.	107.12	4.08720	.03183	.00533	.05656
950.	89.		700000.		
5.	32471.16	1.93330	.00964	.04649	.07553
950.	71.		700000.		
10.	5163.81	2.18113	.01227	.02621	.05788
950.	63.		700000.		
15.	1819.54	2.37034	.01459	.01912	.05312
950.	59.		700000.		
20.	888.10	2.56325	.01688	.01534	.05163
950.	56.		700000.		
25.	511.52	2.72008	.01899	.01301	.05141

950.	53.		700000.		
30.	324.74	2.82008	.02084	.01147	.05171
950.	52.		700000.		
35.	225.32	2.98856	.02296	.01022	.05259
950.	50.		700000.		
40.	162.37	3.07202	.02470	.00936	.05346
950.	49.		700000.		
45.	122.78	3.19320	.02659	.00862	.05461
950.	48.		700000.		
50.	95.59	3.29724	.02840	.00802	.05583
950.	83.		800000.		
5.	28285.83	1.57759	.00840	.06482	.09262
950.	67.		800000.		
10.	4561.82	1.80097	.01084	.03663	.06687
950.	60.		800000.		
15.	1626.75	1.97528	.01305	.02679	.05924
950.	55.		800000.		
20.	787.45	2.09079	.01497	.02178	.05616
950.	53.		800000.		
25.	459.66	2.25257	.01707	.01844	.05491
950.	51.		800000.		
30.	295.75	2.37445	.01898	.01621	.05459
950.	49.		800000.		
35.	203.45	2.46412	.02073	.01462	.05476
950.	48.		800000.		
40.	148.53	2.58050	.02259	.01331	.05531
950.	47.		800000.		
45.	112.52	2.68001	.02437	.01229	.05607
950.	46.		800000.		
50.	87.76	2.76487	.02608	.01147	.05695
950.	79.		900000.		
5.	25527.03	1.33472	.00758	.08751	.11449

950.	63.		900000.		
10.	4095.08	1.50529	.00973	.04979	.07892
950.	57.		900000.		
15.	1477.11	1.66801	.01185	.03646	.06771
950.	53.		900000.		
20.	724.33	1.79089	.01377	.02961	.06278
950.	51.		900000.		
25.	423.72	1.92672	.01573	.02515	.06029
950.	49.		900000.		
30.	273.22	2.02785	.01753	.02219	.05913
950.	47.		900000.		
35.	188.35	2.10093	.01919	.02010	.05869
950.	46.		900000.		
40.	137.75	2.19820	.02095	.01835	.05870
950.	45.		900000.		
45.	104.54	2.28086	.02264	.01698	.05903
950.	45.		900000.		
50.	82.50	2.40424	.02451	.01570	.05961
950.	76.		1000000.		
5.	23612.39	1.15563	.00701	.11542	.14183
950.	61.		1000000.		
10.	3803.58	1.31175	.00904	.06552	.09396
950.	55.		1000000.		
15.	1373.01	1.44854	.01101	.04819	.07860
950.	51.		1000000.		
20.	674.51	1.55098	.01282	.03930	.07153
950.	49.		1000000.		
25.	395.29	1.66605	.01468	.03350	.06759
950.	47.		1000000.		
30.	255.37	1.75057	.01639	.02966	.06545
950.	46.		1000000.		
35.	178.18	1.85060	.01816	.02665	.06421
950.	45.		1000000.		
40.	130.50	1.93537	.01985	.02437	.06363

950.	44.		1000000.		
45.	99.18	2.00715	.02148	.02261	.06349
950.	43.		1000000.		
50.	77.59	2.06764	.02305	.02119	.06365

.01940 20000. .7970

950.	349.		300000.		
5.	245154.44	21.02818	.07284	.00419	.09644
950.	260.		300000.		
10.	34096.33	22.15463	.08105	.00221	.10266
950.	220.		300000.		
15.	10891.91	22.95935	.08738	.00153	.10832
950.	196.		300000.		
20.	4880.33	23.61904	.09281	.00118	.11339
950.	180.		300000.		
25.	2635.28	24.25123	.09788	.00097	.11825
950.	168.		300000.		
30.	1596.51	24.79483	.10246	.00083	.12270
950.	159.		300000.		
35.	1049.39	25.34676	.10695	.00072	.12708
950.	152.		300000.		
40.	731.95	25.90388	.11135	.00065	.13140
950.	145.		300000.		
45.	529.89	26.20991	.11478	.00058	.13477
950.	140.		300000.		
50.	399.50	26.67499	.11871	.00053	.13864
950.	274.		400000.		
5.	151725.79	12.38192	.04508	.00783	.07232
950.	206.		400000.		
10.	21531.33	13.16496	.05118	.00418	.07476
950.	176.		400000.		
15.	7000.65	13.77561	.05616	.00292	.07849
950.	158.		400000.		
20.	3181.32	14.27988	.06049	.00227	.08217
950.	146.		400000.		
25.	1737.88	14.75283	.06454	.00188	.08583
950.	137.		400000.		
30.	1063.53	15.16469	.06826	.00161	.08927

950.	130.		400000.		
35.	704.08	15.54282	.07176	.00141	.09257
950.	124.		400000.		
40.	492.47	15.84908	.07492	.00127	.09559
950.	120.		400000.		
45.	362.17	16.26822	.07845	.00115	.09900
950.	116.		400000.		
50.	274.35	16.57660	.08152	.00105	.10198
950.	230.		500000.		
5.	106808.97	8.31486	.03173	.01283	.06397
950.	174.		500000.		
10.	15397.69	8.89593	.03660	.00691	.06292
950.	150.		500000.		
15.	5085.84	9.39246	.04080	.00487	.06507
950.	135.		500000.		
20.	2331.81	9.76093	.04434	.00381	.06756
950.	126.		500000.		
25.	1291.40	10.18551	04796	.00316	.07053
950.	118.		500000.		
30.	793.11	10.44925	.05090	.00273	.07303
950.	113.		500000.		
35.	531.15	10.80824	.05413	.00240	.07594
950.	108.		500000.		
40.	373.64	11.04323	.05684	.00216	.07840
950.	104.		500000.		
45.	274.74	11.27930	.05951	.00197	.08088
950.	101.		500000.		
50.	209.57	11.54646	.06227	.00181	.08348
950.	200.		600000.		
5.	81070.85	6.02526	.02408	.01936	.06285
950.	153.		600000.		
10.	11904.09	6.51857	.02829	.01051	.05821

950.	132.		600000.		
15.	3963.41	6.88780	.03179	.00745	.05865
950.	120.		600000.		
20.	1843.09	7.23032	.03505	.00586	.06032
950.	112.		600000.		
25.	1025.89	7.54482	.03810	.00489	.06239
950.	106.		600000.		
30.	638.04	7.82218	.04095	.00422	.06457
950.	101.		600000.		
35.	427.38	8.05038	.04355	.00374	.06670
950.	97.		600000.		
40.	302.84	8.26538	.04607	.00337	.06884
950.	94.		600000.		
45.	224.44	8.49562	.04861	.00307	.07109
950.	91.		600000.		
50.	171.34	8.66937	.05091	.00284	.07315

950.	179.		700000.		
5.	65091.78	4.62224	.01934	.02758	.06632
950.	138.		700000.		
10.	9690.85	5.03957	.02303	.01506	.05750
950.	120.		700000.		
15.	3267.95	5.36712	.02621	.01073	.05635
950.	109.		700000.		
20.	1526.97	5.62932	.02903	.00850	.05694
950.	102.		700000.		
25.	855.54	5.88958	.03177	.00711	.05829
950.	97.		700000.		
30.	536.11	6.13545	.03440	.00616	.05997
950.	93.		700000.		
35.	361.99	6.35377	.03689	.00546	.06176
950.	90.		700000.		
40.	258.68	6.57335	.03935	.00493	.06368
950.	87.		700000.		
45.	191.93	6.73969	.04157	.00451	.06549

950.	85.		700000.		
50.	147.81	6.94094	.04392	.00417	.06749
950.	164.		800000.		
5.	54574.94	3.70553	.01621	.03768	.07329
950.	127.		800000.		
10.	8202.20	4.05813	.01949	.02068	.05958
950.	111.		800000.		
15.	2792.58	4.34401	.02240	.01480	.05660
950.	101.		800000.		
20.	1312.97	4.56413	.02496	.01177	.05614
950.	95.		800000.		
25.	741.35	4.79972	.02753	.00987	.05681
950.	90.		800000.		
30.	465.00	4.98110	.02984	.00859	.05784
950.	87.		800000.		
35.	316.71	5.20086	.03227	.00763	.05931
950.	84.		800000.		
40.	226.61	5.36823	.03447	.00691	.06078
950.	81.		800000.		
45.	168.34	5.49052	.03646	.00635	.06221
950.	79.		800000.		
50.	129.80	5.64461	.03857	.00588	.06385
950.	152.		900000.		
5.	47061.30	3.05280	.01398	.04991	.08330
950.	118.		900000.		
10.	7119.64	3.35159	.01692	.02751	.06383
950.	104.		900000.		
15.	2451.30	3.61783	.01966	.01974	.05881
950.	95.		900000.		
20.	1160.79	3.81600	.02207	.01575	.05723
950.	89.		900000.		
25.	656.02	3.99696	.02436	.01328	.05705

950.	85.		900000.					
30.	415.07	4.18166	.02664	.01157	.05761			
950.	82.		900000.					
35.	283.09	4.35730	.02885	.01030	.05856			
950.	79.		900000.					
40.	202.81	4.48773	.03085	.00936	.05962			
950.	77.		900000.					
45.	152.03	4.63945	.03293	.00859	.06092			
950.	76.		900000.					
50.	118.30	4.82690	.03515	.00793	.06248			
950.	143.		1000000.					
5.	41709.07	2.58483	.01239	.06450	.09629			
950.	111.		1000000.					
10.	6328.77	2.83749	.01504	.03566	.07010			
950.	98.		1000000.					
15.	2190.91	3.06820	.01757	.02569	.06266			
950.	90.		1000000.					
20.	1045.41	3.25364	.01988	.02055	.05983			
950.	85.		1000000.					
25.	595.92	3.43559	.02213	.01733	.05886			
950.	81.		1000000.					
30.	377.54	3.58639	.02423	.01514	.05878			
950.	78.		1000000.					
35.	257.84	3.73027	.02627	.01353	.05921			
950.	76.		1000000.					
40.	186.41	3.88558	.02836	.01227	.06003			
950.	74.		1000000.					
45.	139.92	4.01282	.03030	.01129	.06099			
950.	72.		1000000.					
50.	108.16	4.11557	.03213	.01050	.06204			
950.	136.		1100000.					
5.	37768.76	2.23482	.01122	.08174	.11236			

950.	106.		1100000.		
10.	5756.47	2.46334	.01368	.04521	.07829
950.	94.		1100000.		
15.	2005.33	2.67542	.01608	.03263	.06811
950.	86.		1100000.		
20.	957.51	2.82639	.01820	.02621	.06382
950.	82.		1100000.		
25.	550.60	3.01303	.02045	.02209	.06194
950.	78.		1100000.		
30.	349.29	3.13960	.02241	.01937	.06119
950.	75.		1100000.		
35.	238.86	3.26073	.02434	.01736	.06110
950.	73.		1100000.		
40.	172.91	3.39291	.02630	.01577	.06148
950.	71.		1100000.		
45.	129.94	3.50013	.02814	.01454	.06209
950.	70.		1100000.		
50.	101.34	3.63749	.03011	.01347	.06298
950.	131.		1200000.		
5.	34928.06	1.97327	.01037	.10189	.13167
950.	102.		1200000.		
10.	5317.28	2.17285	.01263	.05634	.08838
950.	90.		1200000.		
15.	1850.75	2.34811	.01484	.04083	.07508
950.	83.		1200000.		
20.	890.81	2.50048	.01694	.03281	.06915
950.	79.		1200000.		
25.	512.81	2.66089	.01904	.02773	.06618
950.	75.		1200000.		
30.	325.70	2.76728	.02090	.02439	.06469
950.	73.		1200000.		
35.	224.72	2.90929	.02290	.02178	.06409
950.	71.		1200000.		
40.	162.85	3.02496	.02477	.01983	.06401

950.	69.		1200000.		
45.	122.52	3.11807	.02654	.01832	.06426
950.	68.		1200000.		
50.	95.65	3.23910	.02842	.01699	.06482
950.	127.		1300000.		
5.	32782.43	1.76586	.00974	.12542	.15456
950.	98.		1300000.		
10.	4949.56	1.92706	.01176	.06940	.10057
950.	87.		1300000.		
15.	1733.20	2.09524	.01390	.05029	.08360
950.	81.		1300000.		
20.	840.92	2.25252	.01599	.04035	.07574
950.	76.		1300000.		
25.	480.92	2.36294	.01786	.03437	.07163
950.	73.		1300000.		
30.	308.12	2.48629	.01977	.03014	.06931
950.	71.		1300000.		
35.	212.80	2.61193	.02168	.02697	.06806
950.	69.		1300000.		
40.	154.38	2.71361	.02348	.02459	.06748
950.	68.		1300000.		
45.	117.13	2.83651	.02537	.02259	.06737
950.	66.		1300000.		
50.	90.84	2.90200	.02699	.02114	.06754

Vita

Alfred Harry Davidson III [redacted] the son of Alfred Harry Davidson Jr. and Virginia Stover Davidson. After graduating from Whittier Union High School, Whitter, California, he enlisted in the U. S. Army. Upon his discharge, he entered the United States Military Academy at West Point, New York. He graduated in June 1957 with a degree of Bachelor of Science and a commission in the United States Air Force. His military assignment prior to his work at the Air Force Institute of Technology was as transport pilot with the Military Air Transport Command.

[redacted] [redacted]

Vita

James Franklin Russell [redacted] the son of Monroe Franklin Russell and Marjorie Hicks Russell. After being graduated from Lima Local High School, Summit Station, Ohio, in 1952, he attended the Ohio State University, Columbus, Ohio. In July 1953 he entered the United States Military Academy at West Point, New York, and was graduated in June 1957 with the degree of Bachelor of Science and a commission in the United States Air Force. His military assignment prior to his work at the Air Force Institute of Technology was as missile launch officer in the Strategic Air Command at RAF Feltwell, England.

[redacted] [redacted]

This thesis was typed by Mrs. Nellie Weaver.

UNCLASSIFIED

UNCLASSIFIED